SCIENCE CHINA PRESS

SCIENCE CHINA Chemistry
https://doi.org/10.1007/s11426-025-2929-y

REVIEWS

Earth-abundant cobalt-catalyzed enantioselective C–H functionalizations

Taixin Yang[1†], Yanbo Zhang[1†], Yingchao Dou[1], Dandan Yang[1*] & Jun-Long Niu[1,2*]

[1]Pingyuan Laboratory, College of Chemistry, Zhengzhou University, Zhengzhou 450001, China
[2]State Key Laboratory of Coking Coal Resources Green Exploitation, Zhengzhou University, Zhengzhou 450001, China
†Equally contributed to this work.
*Corresponding authors (email: yangdandan@zzu.edu.cn; niujunlong@zzu.edu.cn)

Received 24 June 2025; Accepted 31 July 2025; Published online 15 October 2025

Abstract Enantioselective C–H functionalization has emerged as an efficient and transformative tool for constructing complex chiral molecules with exceptional step- and atom-economy. While this field was historically dominated by 4d and 5d transition metal catalysts, recent attention has shifted toward cobalt—an earth-abundant, cost-effective 3d transition metal with unique reactivity. Over the past few years, remarkable progress has been achieved in cobalt-catalyzed enantioselective C–H functionalization, primarily through three catalytic systems: (1) low-valent cobalt(I) catalysis, (2) cyclopentadienyl cobalt(III) catalysis, and (3) *in situ* generated cobalt(III) catalysis. This review provides a comprehensive survey of all reported asymmetric cobalt-catalyzed C–H activations proceeding through inner-sphere mechanisms, providing a systematic analysis of synthetic methodologies, reactivity patterns, origins of stereocontrol, mechanistic insights, and future opportunities.

Keywords cobalt, earth-abundant metal, asymmetric catalysis, enantioselective C–H activation, chiral ligand

1 Introduction

Asymmetric synthesis serves as a cornerstone technology for constructing chiral molecules from simple precursors, with extensive applications in pharmaceuticals, natural products, agriculture, and materials science [1–4]. Given its broad utility, the development of efficient asymmetric catalytic methodologies remains a central focus in modern synthetic chemistry. In this context, transition-metal-catalyzed enantioselective C–H functionalization has emerged as a straightforward and transformative strategy, eliminating the need for substrate prefunctionalization and significantly enhancing step and atom economy [5–8]. Over the past decades, significant progress has been made in 4d and 5d transition metal (*e.g.*, Pd, Rh, Ir)-catalyzed enantioselective C–H functionalization, with in-depth insights into catalytic mechanism and stereocontrol mode [9–13]. However, extending this success to earth-abundant 3d metals remains challenging, primarily due to their variable oxidation states, complex coordination geometries, and insufficient mechanistic understanding [14–18].

Cobalt has emerged as a particularly promising 3d transition metal for enantioselective C–H activations [19–24], combining earth abundance with distinctive reactivity derived from its low electronegativity, multiconfigurational spin states, and adaptable coordination geometries (Scheme 1a). The foundation of cobalt-catalyzed C–H activation was laid in 1955 with Murahashi's report [25] on Co-catalyzed aryl imine carbonylation for isoindolinone synthesis, which concurrently marked the first example in the field of C–H activation (Scheme 1b). A few decades later, in 2010, an *in situ*-generated low-valent cobalt-catalyzed, chelation-assisted C–H alkenylation of arylpyridines or imines with alkynes was reported [26]. Since then, remarkable advances have been achieved in cobalt-catalyzed C–H functionalization through the development of diverse cobalt complexes, directing groups, and ligands. In 2013, a seminal study demonstrated high-valent Cp^*Co^{III}-catalyzed C–H bond addition of 2-arylpyridines to polar electrophiles [27]. Thereafter, the first bidentate aminoquinoline-directed cobalt-catalyzed C–H activation/annulation was achieved in 2014, where a commercially available cobalt salt was oxidized *in situ* to an active Co(III) species by $Mn(OAc)_2$ and O_2 [28]. Subsequently, alternative oxidative strategies employing electricity or photosensitizers with O_2, instead of stoichiometric Mn(III) or Ag(I) oxidants, have been developed [29–31]. Despite significant progress in cobalt-catalyzed C–H functionalization, the development of enantioselective variants has lagged behind their racemic counterparts, largely due to difficulties in designing ligands capable of effective stereocontrol. Consequently, recent efforts have increasingly focused on asymmetric transformations, with significant advancements in both low-valent Co^I, and high-valent cyclopentadienyl Co^{III} catalysis (Scheme 1b). The first catalytic mode, pioneered by Yoshikai [32], involves the *in situ* generation of low-valent cobalt(I) catalysts from the reduction of cobalt(II/III) salt, which initiates the asymmetric transformations in the presence of chiral phosphine or *N*-heterocyclic carbene (NHC) ligands. In contrast, building on the success of Cp*Co(III)-catalyzed C–H activation reactions, high-valent cyclopentadienyl (Cp) Co^{III} complexes catalyzed enantioselective C–H activations received considerable attention. In this context, two strategies have emerged: the combination of achiral Cp*Co(III) with chiral carboxylates, as independently developed by Ackermann, Matsunaga, Yoshino and coworkers [33,34]; and the use of chiral $Cp^xCo(III)$ complexes derived from chiral cyclopentadienyl (Cp^x) ligands, as introduced by Cramer's group [35]. Notably, significant advances in cost-effective asymmetric cobalt catalysis have recently emerged following the independent discovery of a simple Co(II)/salicyloxazoline (Salox) system in 2022 [36,37] (Scheme 1b).

Citation: Yang T, Zhang Y, Dou Y, Yang D, Niu JL. Earth-abundant cobalt-catalyzed enantioselective C–H functionalizations. *Sci China Chem*, https://doi.org/10.1007/s11426-025-2929-y

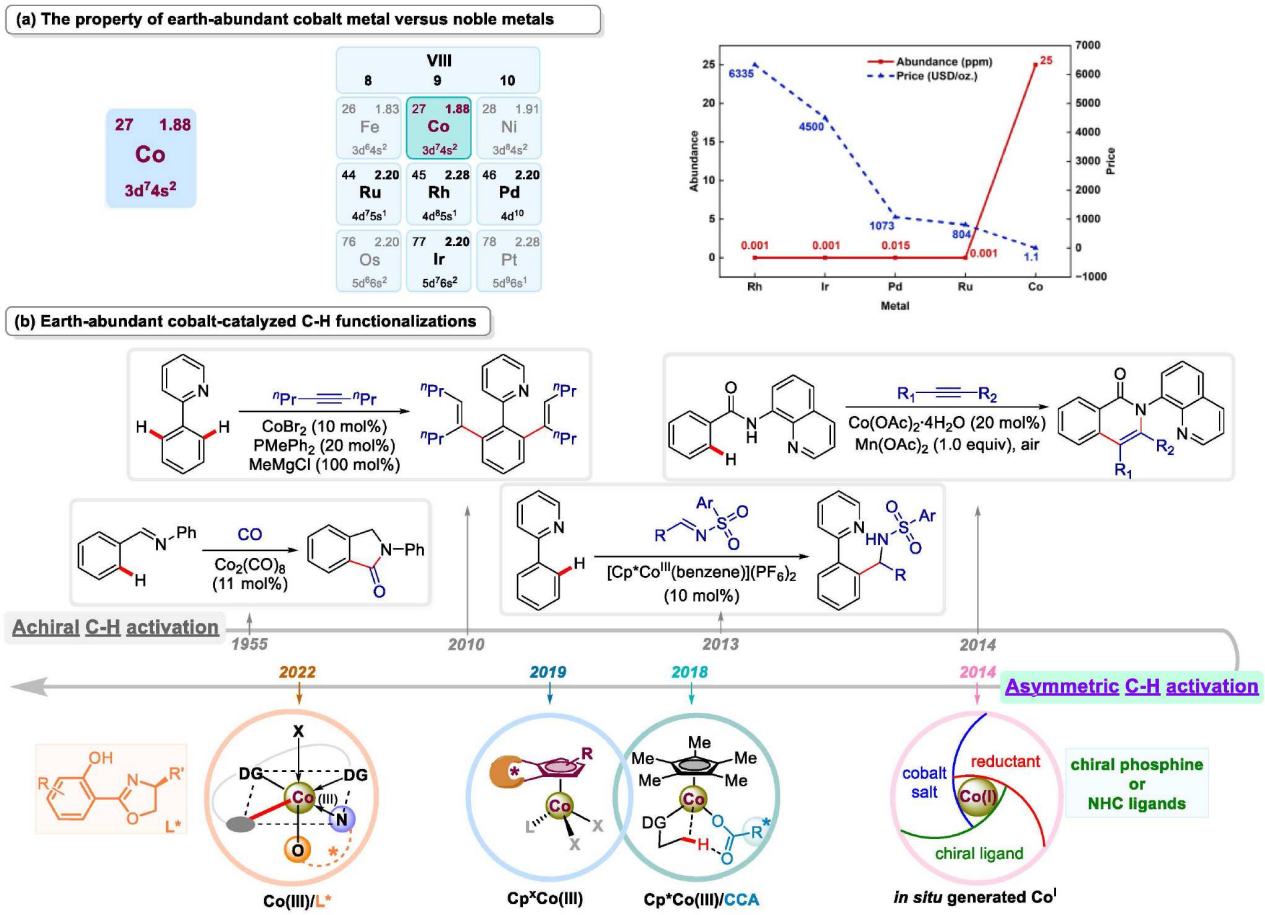

Scheme 1 (Color online) (a, b) Earth-abundant cobalt-catalyzed C–H functionalizations.

Facilitated by a bidentate directing group, this chiral Co/Salox catalytic system has demonstrated remarkable efficacy in constructing diverse stereogenic architectures, including axial, central, planar, inherent, and multiply stereogenic frameworks. Moreover, the successful incorporation of photo- or electrochemical approaches further underscores its robustness and versatility.

In light of these rapid developments, this review aims to provide a timely and comprehensive discussion of cobalt-catalyzed enantioselective C–H functionalizations up to June 2025, focusing specifically on inner-sphere C–H activation mechanisms. And the radical-mediated reactions, such as cobalt porphyrin metalloradical catalysis [38], fall beyond the scope of this discussion. This review is organized based on three mechanistically distinct categories: (1) low-valent cobalt(I) asymmetric catalysis, (2) cyclopentadienyl (Cp) cobalt(III) catalysis, and (3) cobalt(III) catalysis assisted by a bidentate directing group via *in situ* oxidation.

2 Low-valent cobalt-catalyzed enantioselective C–H functionalizations

Low-valent cobalt catalysis, typically comprising a cobalt(II) salt, reductant, and chiral phosphine or *N*-heterocyclic carbene (NHC) ligands, has been successfully employed in enantioselective C–H functionalizations. Mechanistically, the low-valent cobalt catalyst, generated *in situ* via the reduction of cobalt(II) salts in the presence of a reductant and chiral ligand, facilitates the transformation through either: (i) oxidative addition [39] or ligand-to-ligand hydrogen transfer (LLHT) [40] of the C–H bond, or (ii) oxidative cyclization of 1,6-enynes [41,42]. In this respect, the low-valent cobalt-catalyzed enantioselective C–H functionalizations can be classified into the following three categories: hydroacylation of olefins, ketones, or 1,6-enynes; C–H alkylation/arylation of indoles; addition of allylic C–H bonds to ketones.

2.1 Hydroacylation of olefins, ketones, or 1,6-enynes

Based on the structural and mechanistic parallels between rhodium and cobalt in catalytic transformations, the first enantioselective low-valent cobalt catalysis was developed as a viable alternative to conventional rhodium-catalyzed hydroacylations of olefins and ketones [43]. In 2014, Yang and Yoshikai [32] pioneered a cobalt-chiral diphosphine catalytic system for enantioselective intramolecular hydroacylations of 2-acylbenzaldehydes and 2-alkenylbenzaldehydes, yielding phthalide and indanone derivatives, respectively (Scheme 2). Three years later, the same research group extended the applicability of this strategy for the enantio- and diastereoselective intramolecular hydroacylation of trisubstituted alkenes [44] (Scheme 2). The catalytic cycle was proposed to involve: reduction of Co(II) to Co(I), C–H oxidative addition, insertion of the C=X bond into the Co(III)-H bond, and reductive elimination of Co(III) to Co(I) (Scheme 2, bottom).

In 2017, Dong's group [45] disclosed the asymmetric low-valent cobalt catalysis for the construction of enantioenriched cyclobutanones (Scheme 3), marking a significant departure from the traditional rhodium-catalyzed five- or six-membered ring formations [46–48]. The reaction proceeds under mild conditions, demonstrating excellent regio-, diastereo-, and enantioselectivity. Although both Co(0)/Co(II) and Co(I)/Co(III) catalytic cycles are plausible, control experiments support a Co(0)/Co(II) pathway for this cyclization rather than a Co(I)-mediated mechanism.

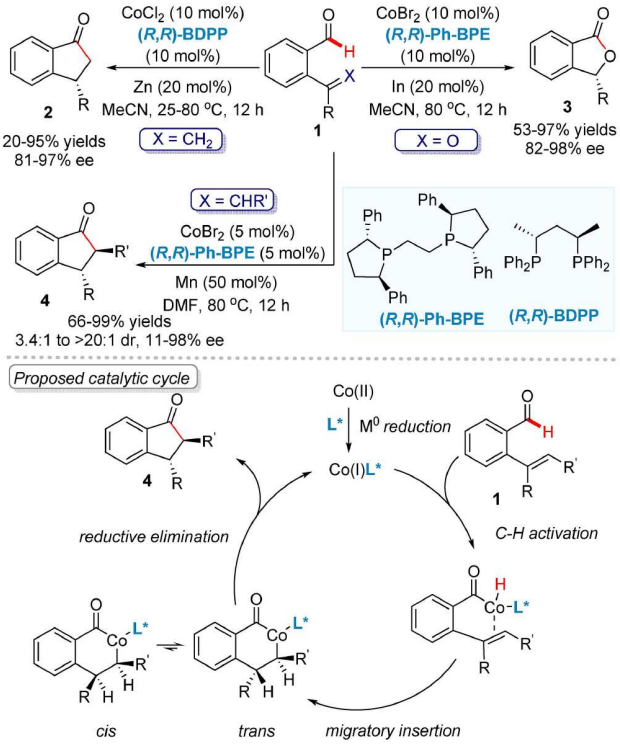

Scheme 2 (Color online) Enantioselective hydroacylations of olefins and ketones.

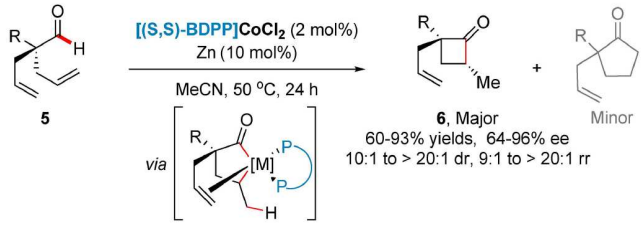

Scheme 3 (Color online) Low-valent cobalt catalysis for enantioselective cyclobutanone construction.

Recently, Liu's group [48] conducted the DFT calculations for understanding the influence of metal centers on the mechanism and chemoselectivity for the transition metal-catalyzed cyclizations of dienyl aldehydes. For both Co(I) and Rh(I) catalysts, the pathway involves oxidative addition and alkene insertion, forming five-membered metallacycles. Electrostatic and orbital interactions critically stabilize these intermediates, dictating chemoselectivity. While Co(I) favors strained cyclobutanones with high enantioselectivity due to lower reductive elimination barriers, Rh(I) preferentially forms cyclopentanones via β-hydride elimination and migratory insertion, facilitated by the stable six-membered rhodacycle.

In 2020, Lautens's group [42] reported the enantioselective cobalt-catalyzed intermolecular hydroacylation of 1,6-enynes **8** with exogenous aldehydes **7** in a domino sequence to construct enantioenriched ketones (Scheme 4). The aromatic substituent (R^2) on the alkyne moiety of 1,6-enynes plays a crucial role in achieving high enantiocontrol. Mechanistic studies indicate no hydrogen crossover occurs. While the reaction likely proceeds through an enantioselective oxidative cyclization pathway, a C–H oxidative addition pathway cannot be excluded. Furthermore, the ligand-controlled divergent C–H functionalization of the aldehyde with enynes in a racemic version was disclosed by Cheng's group [49].

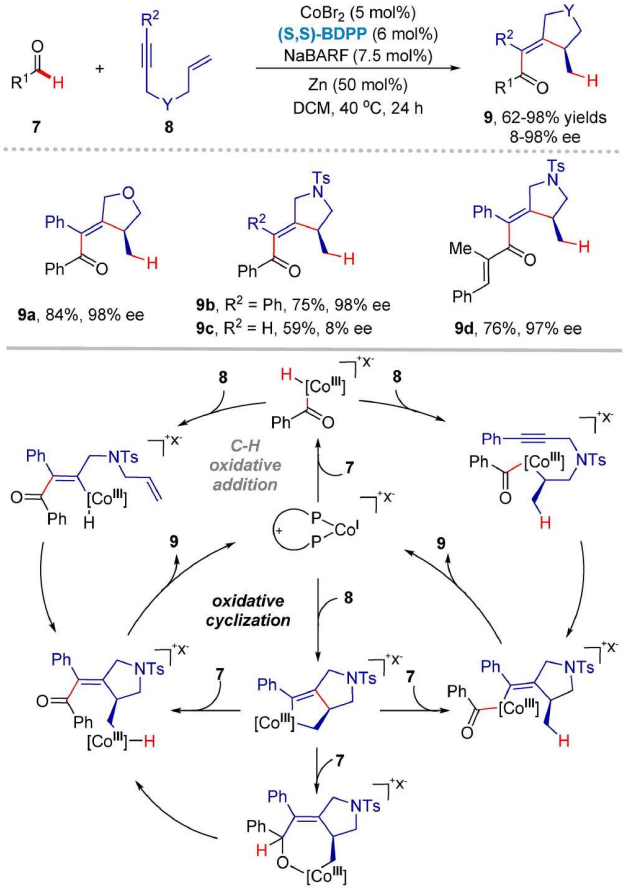

Scheme 4 (Color online) Enantioselective intermolecular hydroacylation of 1,6-enynes.

2.2 C–H alkylation/arylation of indoles

In 2015, Yoshikai and Lee [50] reported an enantioselective cobalt-catalyzed imine-directed C2-alkylation of Boc-protected indoles with styrenes (Scheme 5). The reaction employed a H_8-BINOL derived phosphoramidite as the chiral monophosphine ligand and Me_3SiCH_2MgCl as the reductant, affording 1,1-diarylethane products in 16%–88% yields with 58%–87% ee.

Lautens's group [41] developed a highly enantioselective cobalt-catalyzed C2-alkylation of pyridyl-protected indoles with 1,6-enynes (Scheme 6). The reaction generates two new carbon-carbon bonds and one carbon-hydrogen bond, exhibiting wide substrates scope, good yields and up to 94% ee.

In 2022, Wencel-Delord, Ackermann, and co-workers [51] disclosed an atroposelective C–H arylation of indoles by employing a chiral *N*-heterocyclic carbene (NHC) ligand (Scheme 7). Earlier, in racemic low-cobalt catalysis, Yoshikai's group [52] revealed that the NHC ligand had distinct and complementary reactivities compared to the phosphine ligand. Furthermore, unlike the aforementioned C–H oxidative addition pathway observed in low-cobalt catalysis, this reaction proceeds through a ligand-to-ligand hydrogen transfer (LLHT) pathway to generate key metallacycle species [40]. Subsequently, oxidative addition with 1-chloronaphthalene occurs, followed by reductive elimination, yielding atropoisomeric C2-arylated indoles.

In 2023, Wencel-Delord, Ackermann, and co-workers [53] disclosed a cobalt-catalyzed atroposelective C–H arylation of indoles for the synthesis of atropisomeric indoles bearing vicinal C–C and C–N diaxes in one step (Scheme 8). This transformation demonstrates high reactivity and excellent diastereo- and enantioselec-

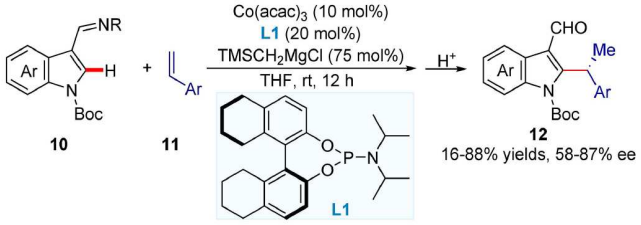

Scheme 5 (Color online) Enantioselective imine-directed C2-alkylation of indoles.

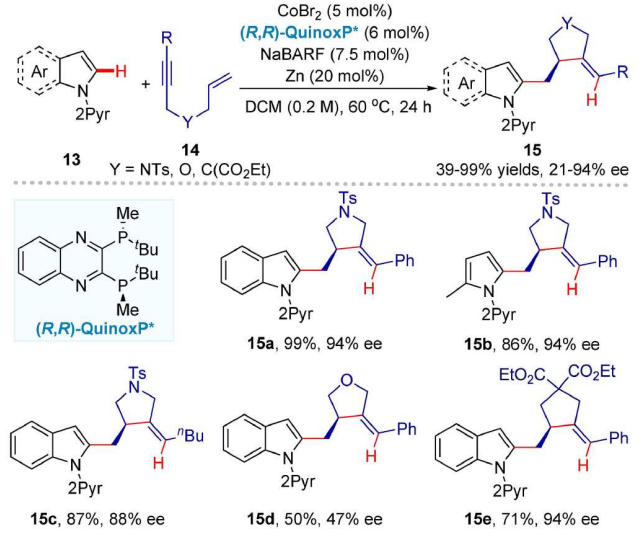

Scheme 6 (Color online) Enantioselective C2-alkylation of indoles with 1,6-enynes.

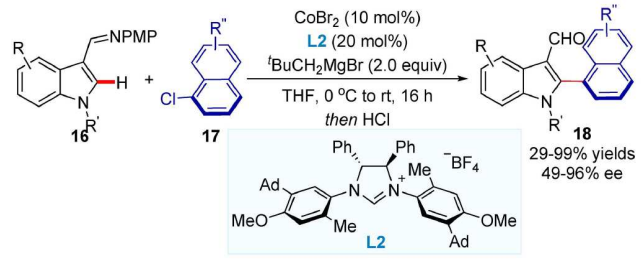

Scheme 7 (Color online) Co/NHC-catalyzed atroposelective C–H arylation of indoles.

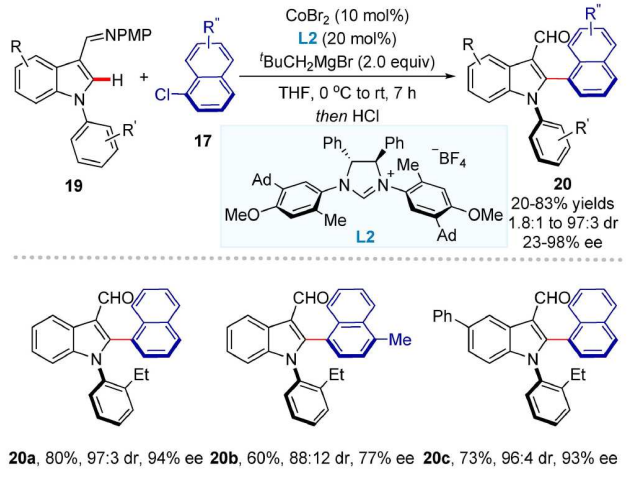

Scheme 8 (Color online) Cobalt-catalyzed C–H activation for the synthesis of C–C and C–N axially chiral indoles.

tivities through the combination of a chiral NHC ligand and a low-valent cobalt catalyst under mild conditions. Racemization experiments and DFT calculations revealed superior atropostability of the C–N axis ($\Delta G^{\ddagger}_{C-N}$ = 33 kcal/mol) compared to the C–C axis ($\Delta G^{\ddagger}_{C-C}$ = 24.9 kcal/mol). Moreover, experimental and theoretical mechanistic investigations suggest that the diastereo- and enantioselectivity originate from dispersive interactions in the oxidative addition transition state coupled with rigorous control of C–N axial chirality during metallation.

2.3 Addition of allylic C–H bonds to ketones

Asymmetric protocols for allylic C–H functionalization via electrophilic η^3-allyl-metal intermediates, enabled by Pd or Rh complexes, have been well developed [54]. In 2017, Sato and Mita [55] developed a low-valent cobalt catalytic system consisting of Co(acac)$_2$, Xantphos, and AlMe$_3$, which facilitated the nucleophilic addition of allylarene C(sp^3)–H bonds to ketones through an active low-valent η^1-allylcobalt(I) species. Notably, using (*R*)-DIFLUORPHOS as the chiral ligand, a single asymmetric example was achieved with 25% yield and 81% ee (Scheme 9).

In 2021, Meng's group [56] reported the diastereo- and enantioselective addition of allylbenzene C(sp^3)–H bonds to aldehydes and α-ketoesters, through low-valent cobalt-catalyzed allylic C–H functionalization (Scheme 10). This transformation exhibits a broad substrate scope, providing homoallylic alcohols in good yields with high stereoselectivity. The synthetic utility of this protocol was further demonstrated by the enantioselective formal synthesis of lithospermic acid and the total synthesis of a pharmaceutical molecule.

3 Cp^{x}Co^{III}-catalyzed enantioselective C–H functionalizations

Since the pioneering studies by Kanai and Matsunaga, high-valent

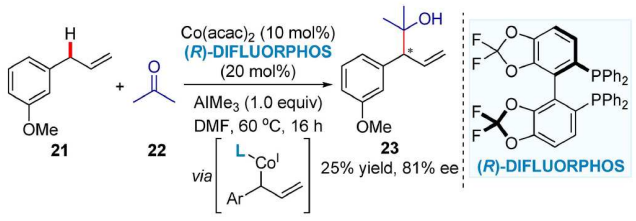

Scheme 9 (Color online) Cobalt-catalyzed addition of allylic C–H bonds to ketones.

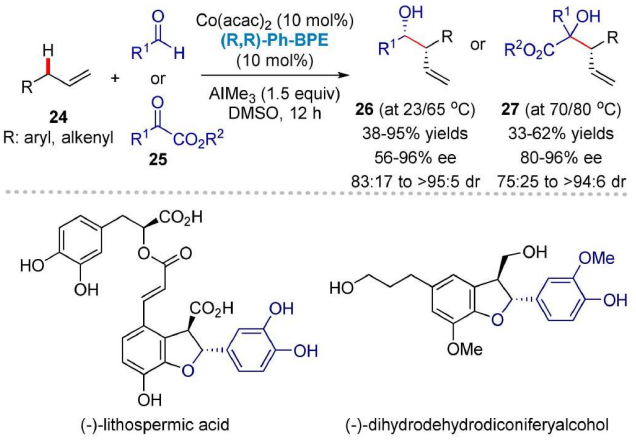

Scheme 10 (Color online) Addition of allylic C–H bonds to aldehydes and α-ketoesters.

cyclopentadienyl cobalt (Cp^*Co^{III}) complexes have emerged as viable alternatives to the cationic Cp^*Rh^{III} catalysts for C–H functionalizations [27], owing to their earth-abundant, cost-efficient, and unique reactivity [57,58]. For the typical high-valent cobalt-catalyzed C–H functionalization, the Cp*Co(III) catalyst facilitates the C–H activation process through a concerted metalation-deprotonation (CMD) mechanism to generate the key active cyclometalated intermediate, which differs significantly from the oxidative addition or ligand-to-ligand hydrogen transfer (LLHT) mechanisms observed in the low-valent cobalt catalysis. In this context, two strategies have been developed for the enantioselective Co^{III}-catalyzed C–H functionalizations: (i) an achiral Cp^*Co^{III} catalyst paired with chiral carboxylic acid (CCA) ligand [12], as reported by Ackermann, Matsunaga and Yoshino, Shi; (ii) a chiral Cp^xCo^{III} system derived from a chiral cyclopentadienyl ligand, as described by Cramer, and You.

3.1 Achiral Cp^*Co^{III}/CCA catalysis

In 2017, Ackermann's group [59] reported a Cp*Co(III)-catalyzed C–H alkylation of indole with an alkene, demonstrating one asymmetric example with a 37% yield and 25% ee by employing Phth-protected L-leucine as the chiral ligand (Scheme 11). This promising result highlights the potential of chiral carboxylic acids for achieving enantioselective control in Cp*Co(III) catalysis. One year later, the same research group established the enantioselective transformation using an achiral Cp*Co(III) catalyst combined with a newly designed C_2-symmetric chiral carboxylic acid [33] (Scheme 11). Notably, the addition of Amberlyst 15 significantly enhanced the reaction performance. In 2019, Matsunaga, Yoshino, and coworkers [60] disclosed a Cp*Co(III)/CAA-catalyzed asymmetric 1,4-addition of indoles to maleimides (Scheme 11). This protocol expanded the scope of alkenes to maleimides by using a BINOL-derived chiral carboxylic acid, albeit with moderate enantioselectivity (10%–64% ee).

Despite these significant advancements, the enantiocontrol was often unsatisfactory when the aliphatic α-alkenes without the π-chelating interaction from the aryl group were used. To address this, Shi, Hong, and coworkers [61] developed a highly enantioselective Cp*Co(III)-catalyzed C–H alkylation of indoles with unactivated terminal alkenes, yielding C2-alkylated indoles in excellent ee values (Scheme 12). The tailor-made design of bulky amino acid ligand and the development of new directing group were essential for the high enantiocontrol (>90% ee for most cases). Mechanistic studies and DFT calculations suggested that the alkene insertion step was involved in the rate- and stereo-determining step, and a typical noncovalent interaction (NCI) between directing group and chiral ligand was responsible for achieving high chiral induction.

In 2023, Ackermann, Hong, and coworkers [62] reported a data-driven strategy for designing chiral carboxylic acids to construct indoles featuring both central and C–N axial chiralities through cobalt catalysis (Scheme 13). Further experimental validation confirmed that the predicted carboxylic acid scaffold demonstrated remarkable stereochemical control in the C–H alkylation, enabling efficient access to structurally diverse indoles with dual stereogenic elements. This work establishes a machine learning-powered platform that accelerates molecular catalysis discovery by extracting latent structure-activity relationships from existing performance statistics.

While Cp*Co(III) catalysis has enabled well-developed enantioselective C(sp^2)–H activation, the more challenging enantioselective C(sp^3)–H activation remains largely unexplored. In 2017, Seayad, Dixon, and coworkers [63] disclosed a Cp*Co(III)-catalyzed achiral C(sp^3)–H amidation of thioamides using dioxazolones, wherein the

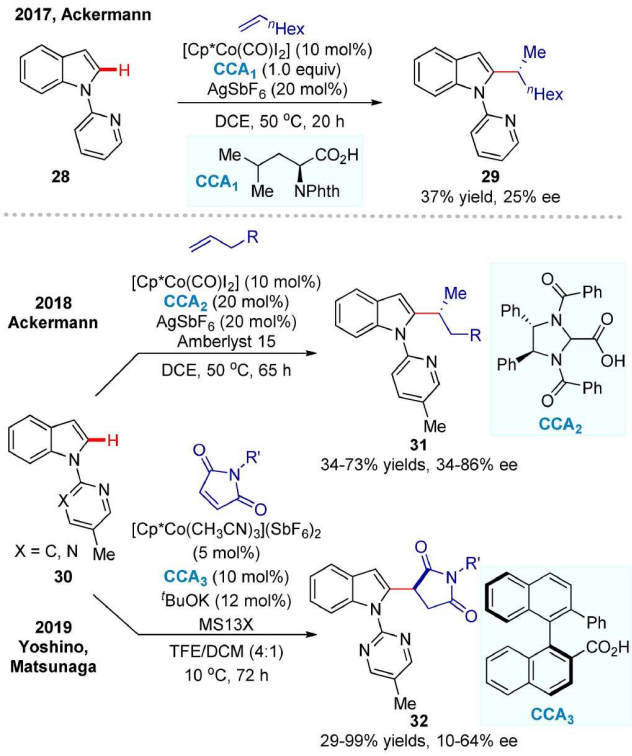

Scheme 11 (Color online) Cp*Co(III)/CCA-catalyzed C–H alkylation of indoles.

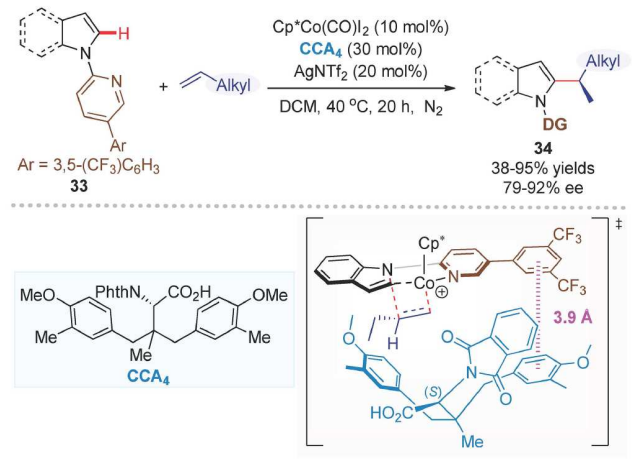

Scheme 12 (Color online) Cp*Co(III)-catalyzed asymmetric C–H alkylation of indoles with unactivated alkenes.

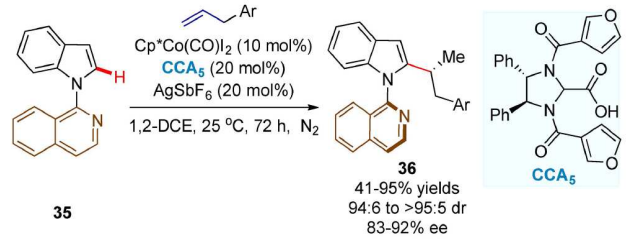

Scheme 13 (Color online) Cp*Co(III)-catalyzed asymmetric C–H activation for the construction of indoles with C-central and C–N axial chirality.

cyclometalation proceeds through an external carboxylate-assisted concerted metalation-deprotonation (CMD) mechanism. Inspired by this work, Matsunaga, Yoshino, and coworkers [34] developed the

first asymmetric variant enabled by an achiral Cp^{x}Co(III) /chiral amino acid derivative system (Scheme 14). The design of sterically more hindered Cp^{x}Co(III) catalyst and the addition of molecular sieves (MS13X) significantly improved the catalytic reactivity and enantioselectivity. This method accommodated a wide range of α-alkyl and α-benzyl thioamides. In addition, mechanistic investigations indicate that the C–H cleavage was irreversible and the C–H activation step determined the enantiocontrol. Subsequently, the same group introduced a new CCA ligand featuring a planar chiral ferrocene backbone, which demonstrated good reactivity and enantioselectivity in Cp*Co(III)-catalyzed C(sp^3)–H amidations of α-aryl thioamide substrates [64] (Scheme 14). And this study complements their earlier findings.

In 2024, Dixon, Hamlin, and coworkers [65] explored a Cp*Co(III)/CCA-catalyzed enantio- and regioselective C(sp^3)–H alkenylation of thioamides with alkynoate esters (Scheme 15). A wide range of alkenylated thioamide products was obtained with high yields and enantioselectivities under mild conditions. Typically, the reaction displayed an unusual regioselectivity rarely observed in such addition of aromatic C–H bonds to alkynes [66,67]. DFT calculations suggested that the enantioselectivity at the C–H activation step and the regioselectivity at the migratory insertion step are both controlled by steric repulsions.

Inspired by the observation that monoprotected amino acids (MPAAs) can promote palladium-catalyzed asymmetric C–H activations [68], Shi's group [69] reported a Cp*Co(III)-catalyzed C–H amidation of ferrocenes using MPAAs as chiral ligands (Scheme 16). The reaction proceeds under mild conditions, providing planar-chiral amidated ferrocenes in high yields with moderate enantiomeric excess. Subsequent recrystallization enhanced the enantiopurity to >99% ee.

Sulfur stereocenters, commonly found in bioactive and pharmacokinetic compounds, typically originate from sulfoxides and sulfoximines [70]. Enantioselective C–H activation has emerged as an efficient method for accessing these chiral compounds [71]. In this context, Matsunaga, Yoshino, and coworkers [72] developed a Cp*Co(III)-catalyzed C–H activation strategy for the asymmetric synthesis of benzothiadiazine-1-oxides via the desymmetrization of diarylsulfoximines (Scheme 17). The design of a new *pseudo*-C_2-asymmetric H_8-binaphthyl chiral carboxylic acid enabled the high enantioselectivity in this transformation. Mechanistic studies and DFT calculations suggested that the irreversible C–H bond cleavage served as both the rate- and enantio-determining step. Shortly thereafter, Shi's group [73] reported a similar study on the synthesis of sulfur-stereogenic sulfoximines (Scheme 17). By employing a chiral monocarboxylic acid ligand derived from (*S*)-BINOL or (*S*)-SPINOL, they achieved the synthesis of a series of chiral cyclic and acyclic sulfoximines with good yields and high enantioselectivities. Notably, the acyclic amidation products can be readily converted into *N*,*S*-chiral sulfoxides. Recently, Matsunaga, Yoshino, and coworkers [74] also reported a Cp*Co(III)/CCA-catalyzed C–H amidation of sulfondiimines, yielding 1,2,4-benzothiadiazine-1imines with high enantioselectivities.

3.2 Chiral Cp^{x}Co^{III} catalysis

In addition to the aforementioned achiral Cp*Co(III) catalyst with an external CCA system, chiral Cp^{x}Co(III) catalysts equipped with chiral cyclopentadienyl (Cp) ligands offer a straightforward strategy for asymmetric C–H functionalizations. However, designing effective and versatile Cp ligands remains a significant challenge. Although several chiral derivatives of the versatile cyclopentadienyl ligands have been applied for the Rh(III)-catalyzed C–H activations, the application in cobalt catalysis remains elusive [75,76]. In 2019,

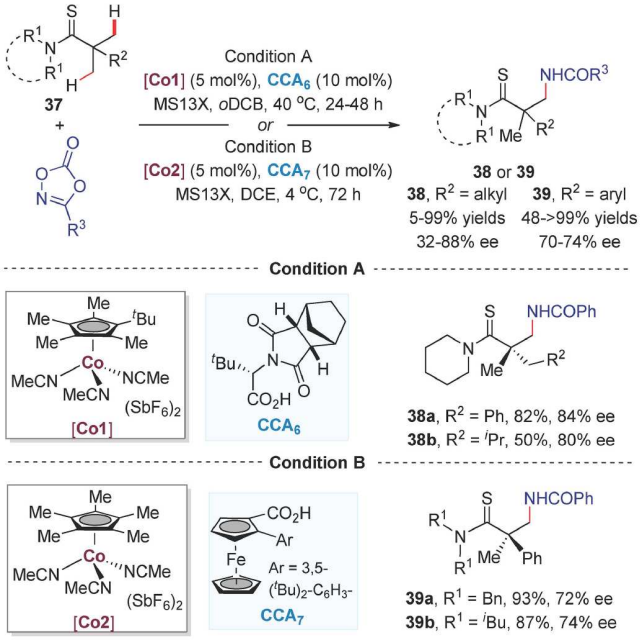

Scheme 14 (Color online) Cp^{x}Co(III)-catalyzed enantioselective C(sp^3)–H amidation of thioamides.

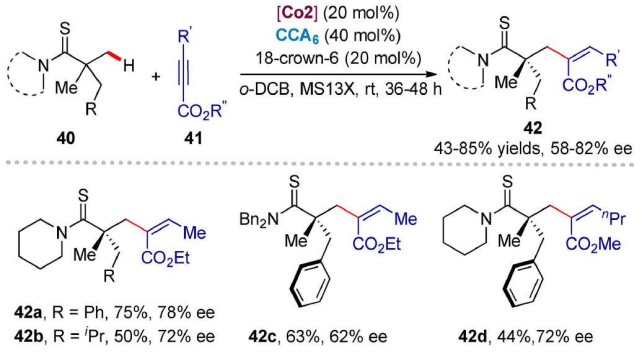

Scheme 15 (Color online) Enantioselective C(sp^3)–H alkenylation of thioamides.

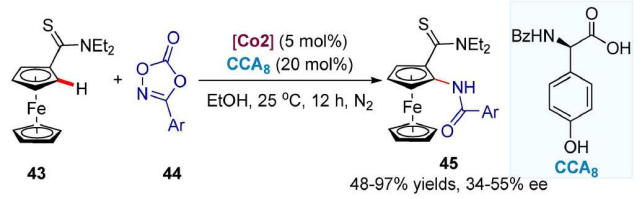

Scheme 16 (Color online) Cp*Co(III)/MPAA-catalyzed enantioselective C–H amidation of ferrocenes.

Cramer's group [35] developed the first class of chiral cyclopentadienyl cobalt(III) complexes featuring trisubstituted chiral Cp^x scaffolds, which demonstrated superior performance for the enantioselective C–H activation/annulation of *N*-chlorobenzamides with alkenes (Scheme 18). The high enantiocontrol stems from the bulky *tert*-butyl sidewall on the Cp^{x}Co(III) complex, which increases the dihedral angle of the biaryl backbone and alters the orientation of the CO ligand, providing an optimal chiral pocket for asymmetric induction. Noteworthy, this cobalt catalytic system exhibits opposite regioselectivity to rhodium catalysis in the annulation of alkyl alkenes [77,78], highlighting that Cp^{x}Co complexes are not merely cheaper and more abundant alternatives to rhodium but

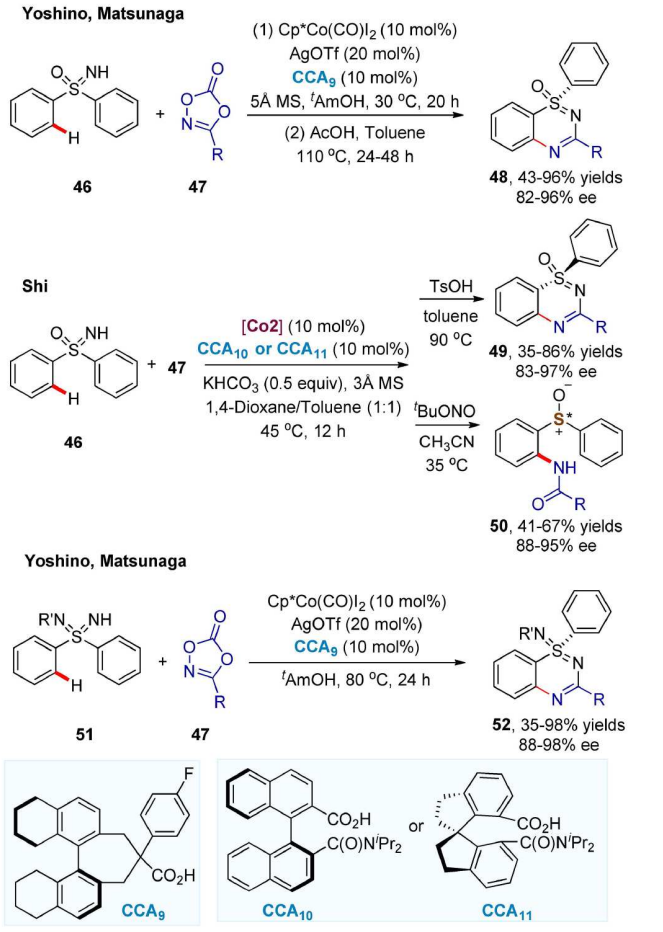

Scheme 17 (Color online) Cp*Co(III)/CCA-catalyzed enantioselective C–H activation to access sulfur stereocenter.

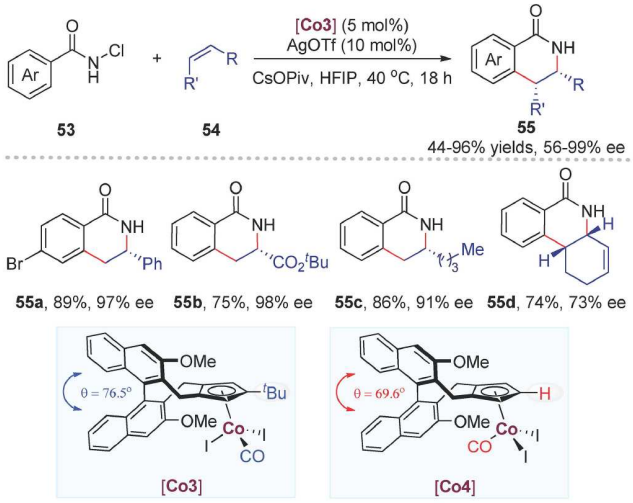

Scheme 18 (Color online) Chiral Cp^{x}Co(III) complex enabled enantioselective C–H/N–H activation/annulation.

uniquely distinct catalysts.

With these chiral Cp^x ligands in hand, Cramer's group [79] turned their attention to the reaction of *N*-phenoxyamides with acrylates or bicyclic olefins [80–82], which reveals the complementary reactivity profile of the Cp*Co(III) catalyst compared to its Cp*Rh(III) congener. They developed a highly enantioselective intermolecular carboamination reaction catalyzed by chiral cyclopentadienyl Co(III) complexes through C–H activation (Scheme 19). This protocol accommodated two distinct alkene acceptors—acrylates and bicyclic olefins, enabling access to valuable unnatural tyrosine derivatives as well as amino-substituted bicyclic scaffolds with excellent enantiocontrol.

Catalytic enantioselective C–H functionalization has emerged as a powerful tool for constructing stereogenic centers. Although its ability to rapidly increase molecular complexity aligns well with multicomponent reactions, achieving such transformations remains highly challenging. In 2016, Ellman's group [83] disclosed the first Cp*Co(III)- and Cp*Rh(III)-catalyzed three-component C–H bond addition cascade, where Cp*Co(III) demonstrated superior diastereoselectivity and broader substrate scope. In 2021, Cramer's group [84] reported the diastereo- and enantio-selective three-component C–H functionalization using a chiral Cp^{x}Co(III) catalyst (Scheme 20). Increasing the bulkiness of the substituent on Cp^x ligand was crucial for both reactivity and high diastereo- and enantioselectivity. Notably, the resulting chiral products displayed opposite diastereoselectivities compared to those obtained with achiral Cp*Co(III) catalysis.

In 2023, You's group [85] developed a Cp^{x}Co(III)-catalyzed asymmetric ring opening (ARO) of 7-oxabenzonorbornadienes through indole C–H functionalization. Notably, the reactions exhibited completely opposite diastereoselectivity compared to the Cp*Co(CO)I_2-catalyzed system [86] (Scheme 21). Combined experimental and computational studies revealed that *cis*- and *trans*-β-oxygen elimination serve as the selectivity-determining steps for the enantioselective and racemic pathways, respectively. Furthermore, the group successfully extended this Cp^{x}Co(III) catalysis to 7-

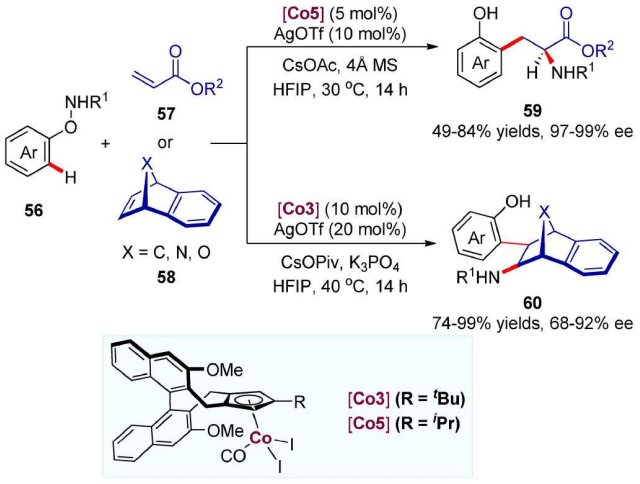

Scheme 19 (Color online) Enantioselective carboamination of *N*-phenoxyamides with acrylates or bicyclic olefins.

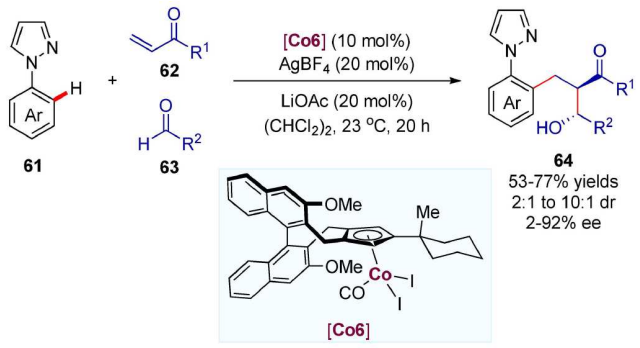

Scheme 20 (Color online) Enantioselective three-component C–H functionalization.

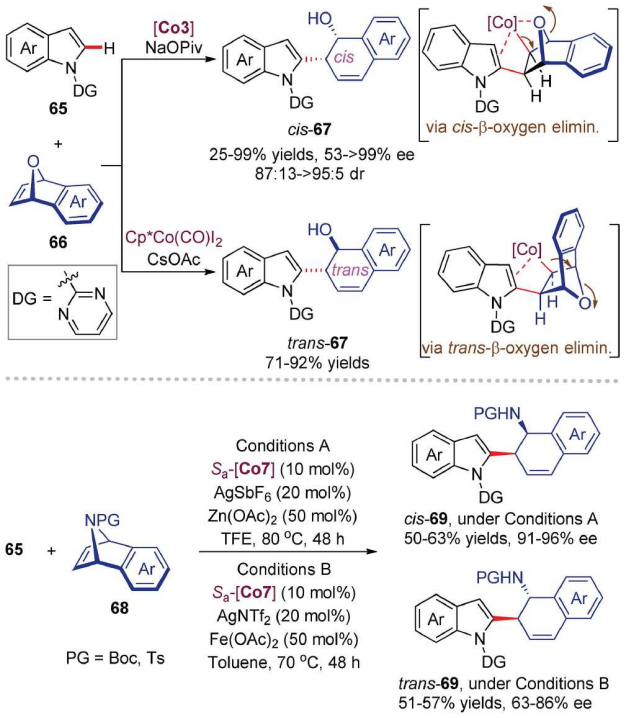

Scheme 21 (Color online) Asymmetric ring-opening of bicyclic olefins via Co-catalyzed C–H activation of indoles.

azabenzonorbornadienes, achieving diastereodivergent ARO reactions.

In 2024, You's group [87] developed an efficient $Cp^xCo(III)$-catalyzed C–H allylation of ferrocene thioamides for constructing planar chiral ferrocene derivatives [54] (Scheme 22). Mechanistic investigations, including control experiments, characterization of key Cp^xCo intermediates, and DFT calculations, revealed that: (1) the C–H cleavage is reversible, and (2) migratory insertion of the C–Co bond into the olefin serves as both the rate- and enantio-determining step. Moreover, the synthetic utilities of this method were highlighted by diverse product transformations and the preparation of a new phosphine-olefin ligand suitable for Rh-catalyzed asymmetric (conjugated) addition reaction.

Recently, Cramer's group [88] reported an enantioselective $Cp^xCo(III)$-catalyzed [4 + 1] annulation of benzamides using cyclopropenes as the one-carbon synthons (Scheme 23). When the same chiral Cp^x ligand was employed in a Rh(III) complex, however, the reaction yielded a [4 + 2] annulation product without any cyclopropane ring opening. This observation highlighted again the distinct and complementary reactivity of Co(III) compared to its Rh(III) homologue [89]. Furthermore, the computational mechanistic studies suggested that the [4 + 1] annulation might proceed via C–H activation of *N*-chlorobenzamide, coordination/migratory insertion of olefin, ring opening of cyclopropane, oxidative addition to form a Co-nitrene intermediate, nitrene insertion and finally Co-N protonation.

4 Asymmetric cobalt(III) catalysis assisted by a bidentate directing group via *in situ* oxidation

In 2014, Daugulis and coworkers [28,90] reported the first bidentate aminoquinoline-directed, cobalt-catalyzed C–H functionalization, where the active Co(III) species was generated *in situ* from a readily available Co(II) salt in the presence of oxygen and Mn $(OAc)_2$. However, achieving an asymmetric version has long

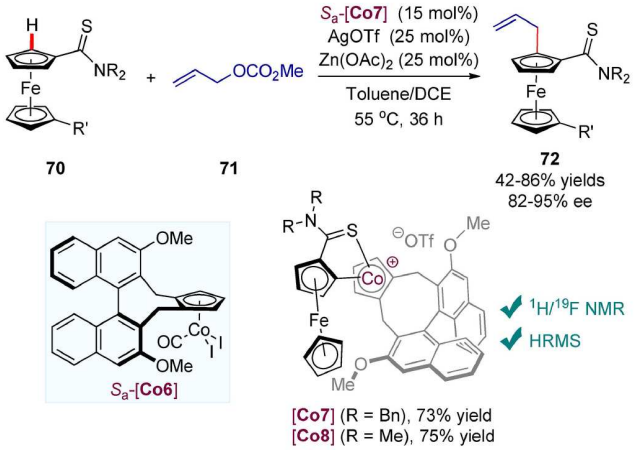

Scheme 22 (Color online) $CpCo^X(III)$-catalyzed C–H allylation of ferrocene thioamides.

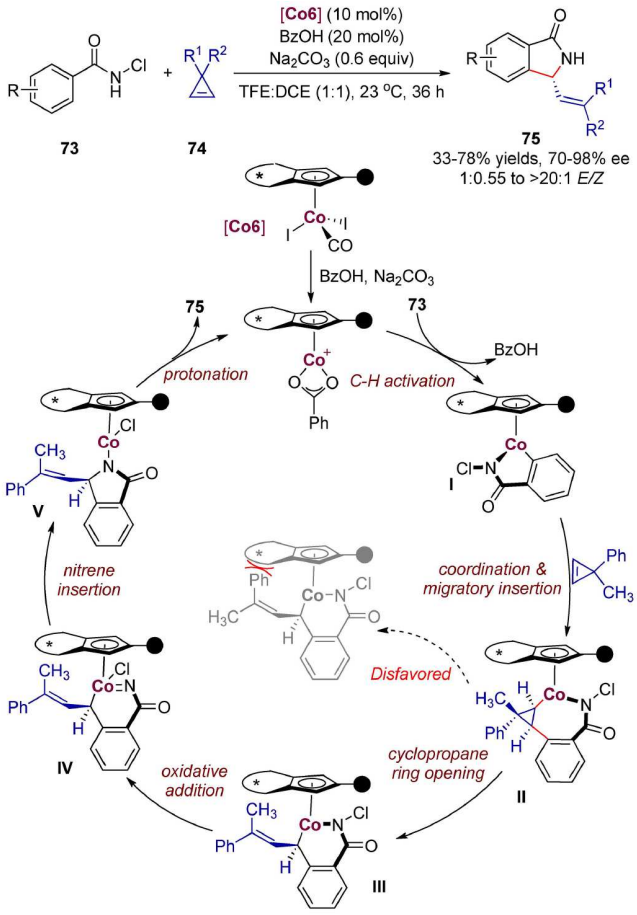

Scheme 23 (Color online) $Cp^xCo(III)$-catalyzed [4 + 1] annulation of benzamides with cyclopropenes.

remained elusive, presumably owing to the structural complexity of the *in situ* generated octahedral Co(III) catalyst (Scheme 24). To this end, the rational design of a chiral ligand represents a promising strategy to achieve the enantioselective C–H functionalization.

In 2021, Shi's group [91] developed a typical cobalt(II)/chiral spiro phosphoric acid (SPA) binary system and demonstrated its activity for the enantioselective synthesis of spiro-γ-lactams through a sequential C–H olefination/asymmetric [4 + 1] spirocyclization (Scheme 25). A series of *N*-quinolinyl arylamides and maleimides was well tolerated in moderate to good yields and high enantioselectivities. Furthermore, the readily removable 5-methoxyquino-

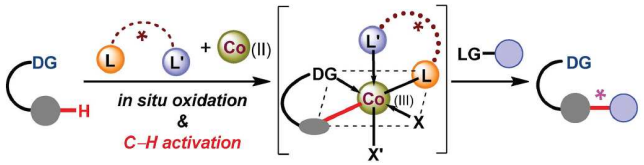

Scheme 24 (Color online) Challenges in Co(III)-catalyzed enantioselective C–H activation.

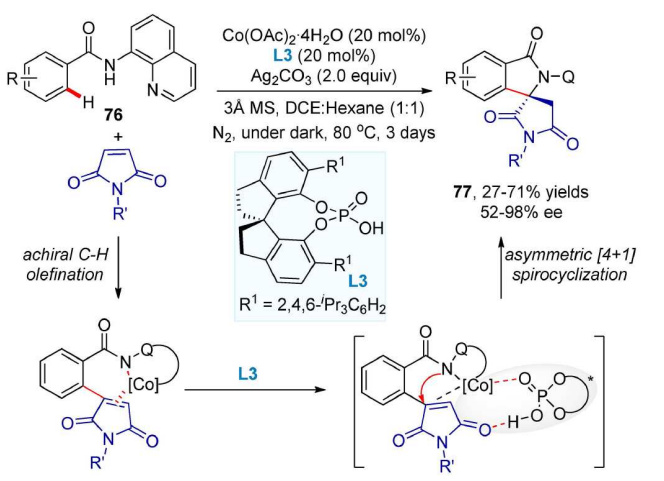

Scheme 25 (Color online) Co/SPA-catalyzed sequential C–H olefination/asymmetric [4 + 1] spirocyclization.

lin-8-amine (MQ) directing group was also compatible with this transformation, underscoring the practical utility of the method. Notably, mechanistic studies indicated that the enantiocontrol was determined in the [4 + 1] spirocyclization, rather than the common C–H activation. Despite this significant advance, cobalt(III) catalysis via *in situ* oxidation still faces unresolved fundamental challenges.

With the growing interest in earth-abundant cobalt catalysis, Shi's group [37] and our group independently established an aminoquinoline-directed, cobalt-catalyzed enantioselective C–H activation/annulation by designing a monoanionic chiral salicyl-oxazoline (Salox) ligand, enabling the construction of C–N axially chiral and *P*-stereogenic chiralities [36,37]. This chiral Salox ligand, which can be readily synthesized in a single step from salicylic acid and amino alcohols in high yields, not only stabilizes the active octahedral Co(III) intermediate but also offers excellent modularity for structural optimization (Scheme 26). Since then, the Co/Salox-catalyzed enantioselective C–H functionalization has been extensively developed to construct axial, central, planar, inherent and multiple chiralities.

4.1 Construction of axial chirality

4.1.1 C–N axial chirality

C–N axially chiral units are important motifs in natural products, bioactive compounds, chiral ligands, and functional materials. While various synthetic approaches exist—including N–H functionalization, chiral C–N axis construction, and desymmetrization—the *de novo* formation of N-heterocycles via direct C–H activation with enantiocontrol remains both appealing and challenging [92–96]. In 2022, our group developed an atroposelective cobalt/Salox-catalyzed C–H/N–H activation/annulation to construct C–N axially chiral frameworks, by installing a sterically hindered group at C7 of the quinoline moiety [36,97,98] (Scheme 27). This Cp-free cobalt catalytic system, consisting of $Co(OAc)_2{\cdot}4H_2O$ with a chiral Salox

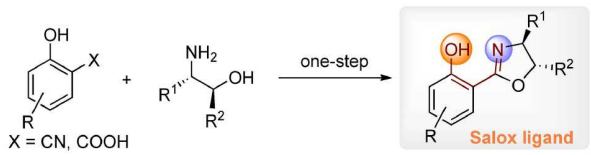

Scheme 26 (Color online) Synthesis of salicyl-oxazoline (Salox) ligand.

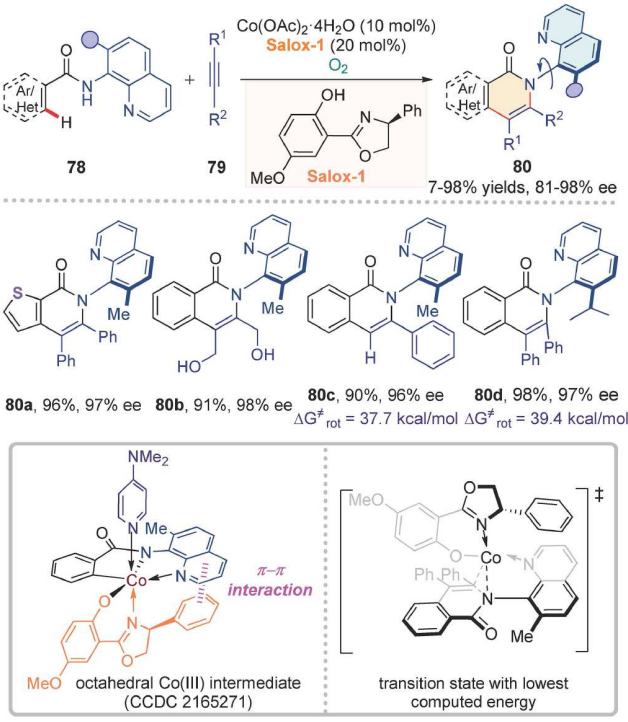

Scheme 27 (Color online) Co/Salox-catalyzed enantioselective C–H activation/annulation to construct the C–N axially chiral framework.

ligand, employs environmentally benign O_2 as the sole oxidant without requiring additives. A broad range of benzamides and internal/terminal alkynes were well tolerated, affording products in high yields and enantioselectivities. The resulting C–N axially chiral isoquinolinones feature remarkable atropostabilities, with rotational barriers reaching 39.4 kcal/mol. Notably, the isolation of a key octahedral cyclometalated Co(III) intermediate, combined with DFT calculations, revealed that the C–N reductive elimination step is stereo-determining. Furthermore, π-π stacking interactions between the phenyl ring of the Salox ligand's oxazoline moiety and the quinoline unit of the benzamide substrate were crucial for high enantiocontrol.

Subsequently, we developed an atroposelective synthesis of five-six heterobiaryl C–N axially chiral compounds via Co/Salox-catalyzed C–H activation [99] (Scheme 28). By employing isonitrile as a unique C1 source, the [4 + 1] cycloaddition-type annulation was achieved in high yields and excellent enantioselectivities. Furthermore, using the allenes as coupling partners, the Co/Slaox-catalyzed atroposelective C–H/N–H activation/annulation was also developed by our group [100] (Scheme 28). With 5 mol% $Co(OAc)_2{\cdot}4H_2O$ as the catalyst, the reaction proceeded through regioselective annulation across two distinct C=C double bonds, efficiently constructing C–N axially chiral frameworks with excellent reactivity and enantiocontrol. Notably, all these Co/Salox-catalyzed protocols employ O_2 as the sole oxidant without requiring any additives, demonstrating the remarkable efficiency of

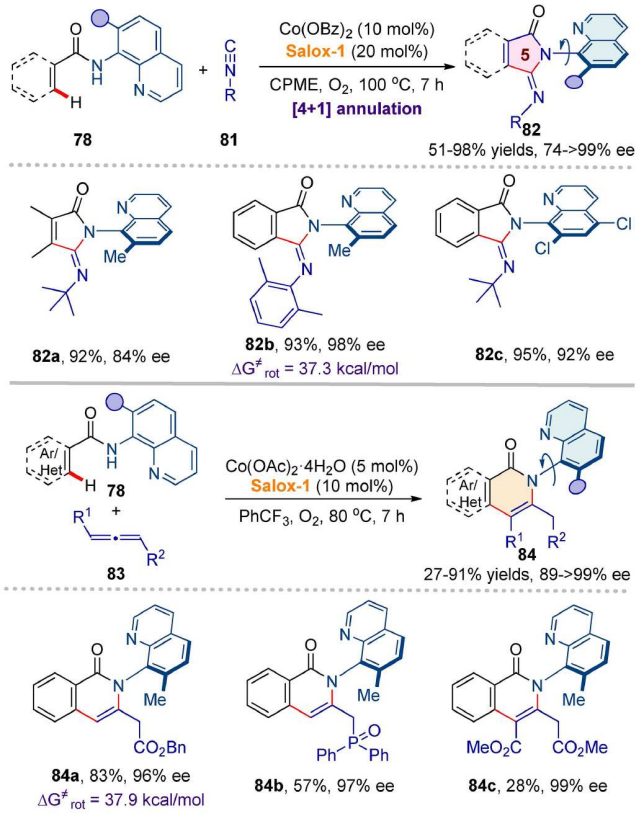

Scheme 28 (Color online) Co/Salox-enabled the construction of the C–N axially chiral framework.

Scheme 29 (Color online) Co/Salox-catalyzed intramolecular C–H annulation to construct atropisomers with vicinal C–C and C–N diaxes.

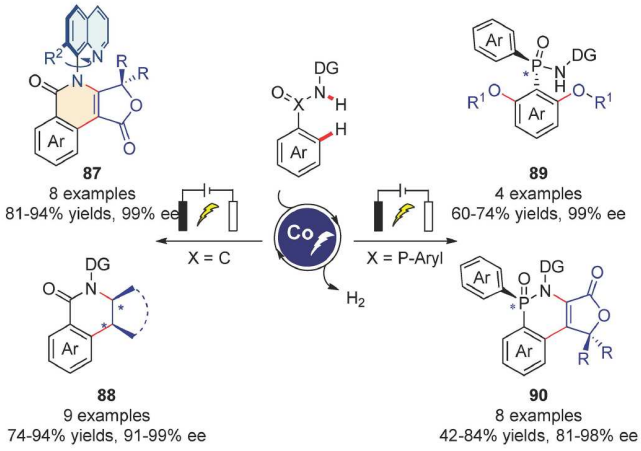

Scheme 30 (Color online) Enantioselective electrochemical cobalt-catalyzed C–H activations.

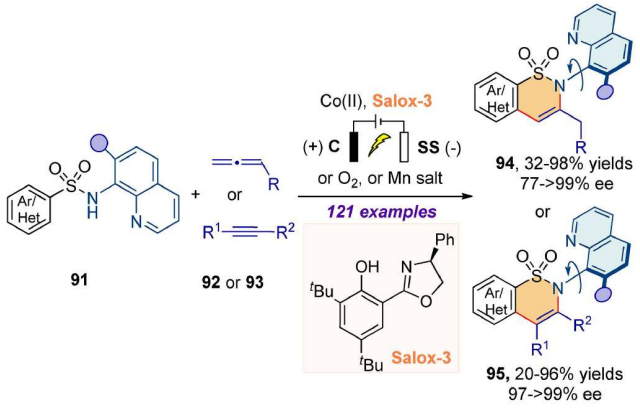

Scheme 31 (Color online) Enantioselective C–H activation of aryl sulfonamides.

this newly established asymmetric Co/Salox system.

In 2022, Shi's group [101] developed a Co/Salox-catalyzed intramolecular atroposelective C–H annulation, efficiently constructing diaxial atropisomers with vicinal C–C and C–N chiral axes [102] (Scheme 29). This protocol utilized $Mn(OAc)_3{\cdot}2H_2O$ as the oxidant and $PivONa{\cdot}2H_2O$ as the base to facilitate C–H activation, delivering high yields with high stereoselectivity and enantioselectivity (up to >99% ee and 70:1 dr). Notably, products bearing large conjugated aryls displayed circularly polarized luminescence (CPL) activity ($|g_{lum}| = 7.0 \times 10^{-4}$). Atropisomerization studies and DFT calculations suggested that the C–N rotational barriers were similar in magnitude and influenced by the *ortho*-substituent bulkiness of the C–C axis, while the C–C rotational barrier varied significantly with steric hindrance at the *ortho* position.

In recent years, organic electrochemistry has emerged as an environmentally benign and synthetically versatile platform, enabling diverse transformations through hydrogen evolution reaction (HER) as an alternative to chemical oxidants [103,104]. In 2023, Ackermann's group [105] reported the enantioselective electrochemical cobalt-catalyzed C–H activation reactions (Scheme 30). Thus, Co/Salox-catalyzed C–H/N–H annulations of benzamides with alkynes afforded C–N axially chiral compounds, while the analogous reaction with alkenes provided access to *C*-stereogenic molecules. Furthermore, the group achieved the desymmetrization of phosphinic amides via electrochemical dehydrogenative C–H alkoxylation and C–H/N–H annulation, following the prior report on *P*-stereogenic compound construction by Shi's group [37].

Our group developed a cobalt-catalyzed enantioselective C–H activation of aryl sulfonamides, providing efficient access to C–N axially chiral sultam derivatives [106] (Scheme 31). This transformation exhibited excellent functional group tolerance (121 examples), accommodating various internal/terminal alkynes and allenes (such as 2,3-butadienoate, allenylphosphonate, and phenylallene) with high regio- and enantioselectivity. Remarkably, the oxidative C–H/N–H annulation with alkynes was successfully achieved under electrochemical conditions, using a simple undivided cell equipped with a carbon cloth (C) anode and a stainless steel (SS) plate cathode.

Significant progress has been made in 8-aminoquinoline (AQ)-directed Co/Salox-catalyzed enantioselective C–H functionalizations. Alternatively, 2-aminopyridine 1-oxide (PyO-amine) bidentate auxiliary first developed by our group [107], has been recognized as one of the most versatile and efficient directing groups for cobalt-catalyzed C–H activations [108,109]. In this context, our group has developed a cobaltaelectro-catalyzed atroposelective C–H annulation strategy enabled by an *N*,*O*-auxiliary [110] (Scheme 32). This approach combines electro-

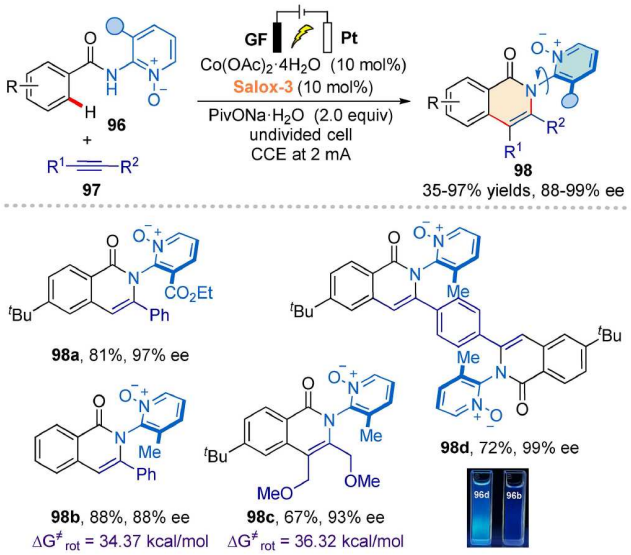

Scheme 32 (Color online) *N*,*O*-auxiliary enabled cobaltaelectro-catalyzed atroposelective C–H annulation.

chemical synthesis with a simple Co/Salox catalytic system, allowing precise control over the chemo- and enantioselectivity of the annulation process. As a result, a series of C–N axially chiral pyridine *N*-oxides was synthesized with good yields and high enantioselectivities. Interestingly, when 1,4-diethynylbenzene was used, the C–N diaxially chiral product, featuring two alkynyl groups participating in the annulation, was isolated in 72% yield with 99% ee. Notably, this product **98d** exhibited enhanced fluorescence emission compared to product **98b**, validating the promising potential of this strategy for developing functional materials.

Despite the aforementioned advances, the asymmetric construction of atropisomers featuring multiple C–N axes remains largely underexplored. Recently, Shi's group [111] reported an atroposelective synthesis of diaxially chiral frameworks bearing both six-five and six-six C–N axes via cobalt-catalyzed atroposelective C–H annulation (Scheme 33), building upon Feng *et al.*'s report [112] on the racemic variant of this transformation. By designing and synthesizing *N*-arylindole-3-carboxamide substrates, the reaction yields a diverse array of chiral pyridoindolone derivatives in high yields with excellent atroposelectivity and diastereoselectivity (most cases >20:1 dr). The isolation of a key octahedral cobalt complex, along with control experiments, suggested that the stereochemistry of both C–N axes was established and fixed simultaneously during the C–H cyclometalation step, facilitated by sufficient steric hindrance. Typically, the representative product **101a** exhibits a high photoluminescence quantum yield (>99%), and product **101c** displays a weak circularly polarized luminescence (CPL) signal ($|g_{lum}| = 1.5 \times 10^{-4}$). These findings underscore the promising potential of this strategy for applications in organic optoelectronic materials.

During the same period, both Ackermann's group [113] and our group [114] independently reported cobalt-catalyzed atroposelective C–H/N–H activation/annulation of benzamides with 2-substituted 1-alkynylindoles, constructing two remote C–N chiral axes in a single step (Scheme 34). In Ackermann's work, the reaction underwent efficiently under electrooxidative conditions using a κ^2-*N*,*O*-oxazoline urea ligand (Scheme 34, Conditions A). The octahedral cyclometalated cobalt(III) complex was isolated, revealing an *N*,*O*-coordination pattern of the chiral ligand analogous to that observed in Salox ligands. DFT calculations identified migratory insertion as the rate-determining step, with the

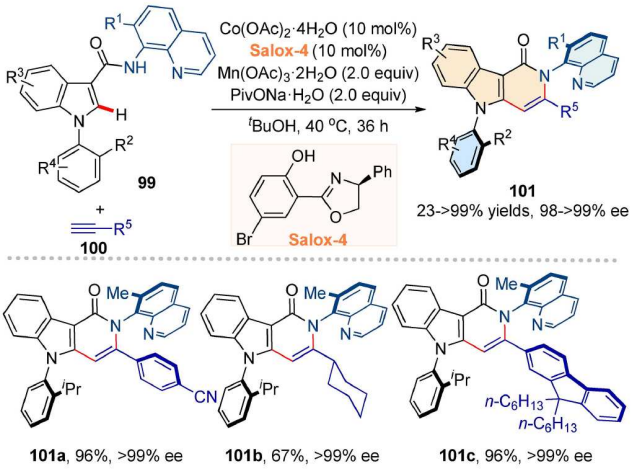

Scheme 33 (Color online) Co/Salox-enabled the construction of multiple C–N axes.

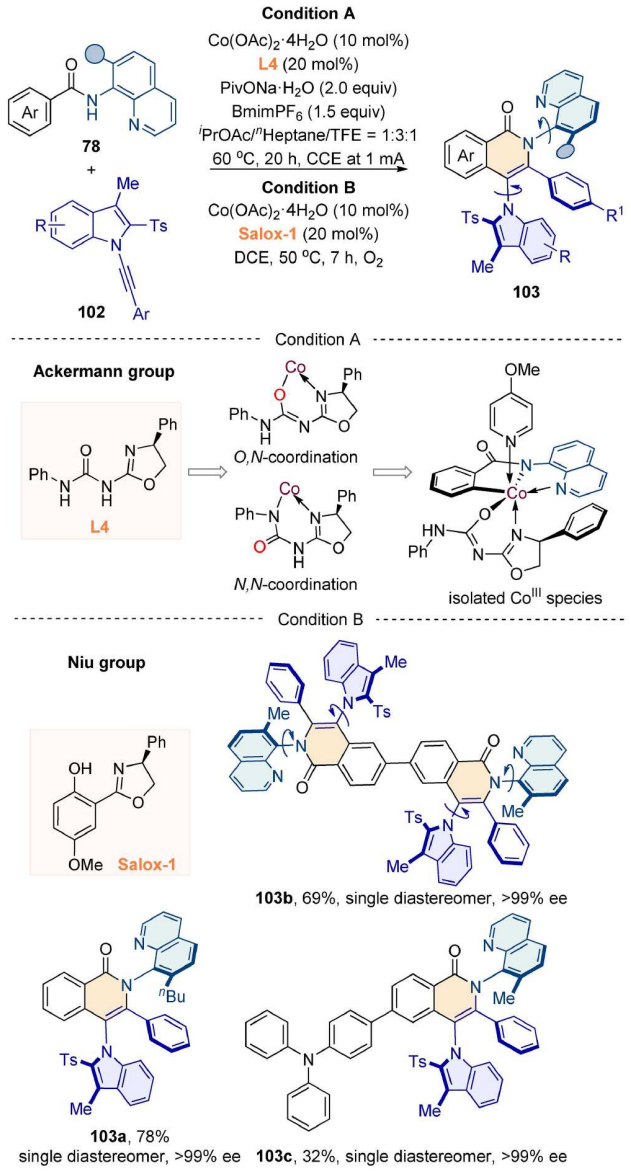

Scheme 34 (Color online) The construction of remote two C–N chiral axes.

O,*N*-coordination mode being energetically favored over *N*,*N*-coordination. In our work, the reaction proceeded under an O_2

atmosphere using $Co(OAc)_2·4H_2O$ catalyst with a chiral Salox ligand (Scheme 34, Conditions B). The resulting atropisomers exhibited exceptional configurational stability, with calculated rotational barriers of 43.2 kcal/mol (on quinoline unit) and 35.8 kcal/mol (on indole unit). Remarkably, the benzamide substrate that contains two amide moieties also underwent smoothly under this protocol, affording **103b** (69% yield, 99% ee) as a single diastereomer with four C–N stereogenic axes. Control experiments confirmed the necessity of a C2-substituent on indole, as no product formed without this sterically hindering group. Unlike the previous Co/Salox system for constructing mono-stereogenic elements, this protocol displays a positive nonlinear effect, suggesting the involvement of multiple Salox-ligand-coordinated cobalt species in the catalytic cycle. Notably, product **103c** features an extremely high fluorescence quantum yield of up to 99%, highlighting its promise for chiral optoelectronic applications.

Very recently, Sundararaju's group [115] also reported an efficient cobalt/Salox-catalyzed method for synthesizing atropisomers featuring distal 1,3-C–N diaxes through C–H/N–H annulation of benzamides with sterically hindered alkynes (Scheme 35). This step-economical, one-pot transformation proceeds at room temperature using O_2 as the sole oxidant. The protocol accommodates a wide range of arylamides and alkynes, delivering high yields and exceptional enantioselectivity (up to >99% ee). Mechanistic investigations, including experimental and DFT studies, reveal that migratory insertion governs the rate-determining step, whereas C–H activation controls enantioselectivity. Furthermore, a traceless bidentate directing group strategy is demonstrated, enabling the construction of C–N atropisomers with high stereocontrol.

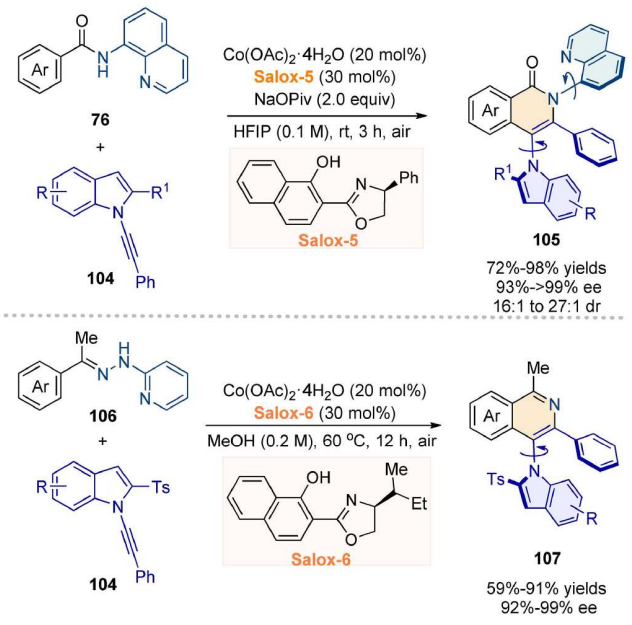

Scheme 35 (Color online) Cobalt-catalyzed asymmetric C–H activation for the construction of C–N Atropisomers.

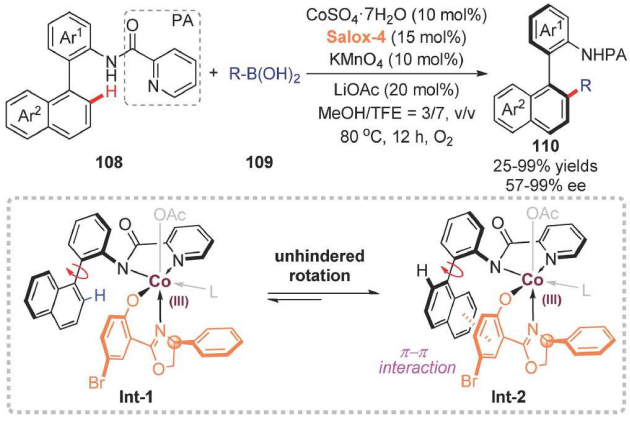

Scheme 36 (Color online) Co/Salox-catalyzed atroposelective C–H arylation to construct C–C axis.

4.1.2 *C–C axial chirality*

Shi's group [116] developed a Co/Salox-catalyzed atoposelective transannular C–H arylation for the synthesis of C–C axially chiral biaryl amines (Scheme 36). The transformation proceeded via a dynamic kinetic asymmetric transformation (DYKAT) manner, exhibiting broad substrate scope, good yields and high enantioselectivities. They proposed that the π-π stacking interactions between the naphthyl group of **108** and the phenolate moiety of **Salox-4** might be critical for the DYKAT process by facilitating unhindered rotation of the biaryl axis from **Int-1** to **Int-2**.

4.1.3 *N–N axial chirality*

While significant progress has been made in C–C and C–N atropisomers in recent years, N–N atropisomerism has long been overlooked, likely due to misconceptions about the stability of N–N axes toward deplanarization. To address this challenge, we developed an efficient Co/Salox-catalyzed system for atroposelective construction of N–N axially chiral frameworks via enantioselective C–H activation/annulation [117] (Scheme 37). Using *N*-(7-azaindole)benzamide as the substrate, inexpensive $Co(OAc)_2·4H_2O$ as the catalyst, **Salox-3** as the chiral ligand, and O_2 as the oxidant, the reaction afforded a range of N–N axially chiral products with high efficiency and enantioselectivity. Racemization experiments and DFT calculations revealed high rotational barriers (>40 kcal/mol) for these N–N atropisomers. Furthermore, a monophosphine ligand incorporating the chiral N–N axis proved highly effective in the Tsuji-Trost reaction, achieving the product in 95% yield with 93% ee. Notably, the transformation also proceeded effectively under electrochemical conditions while retaining excellent enantioselectivity. Building on these findings, we developed a cobalt-electrocatalyzed atroposelective C–H activation/annulation of benzamides with allenes in a simple undivided cell [118] (Scheme 37). The electrochemical protocol accommodated diverse allenes (particularly internal allenes) and functionalized benzamides, efficiently producing N–N axially chiral isoquinolinones in good yields with excellent regio- and enantioselectivity.

Subsequently, Zeng and coworkers [119] reported an electrochemical cobalt-catalyzed atroposelective C–H annulation to construct N–N axially chiral isoquinolinones with high efficiency and enantioselectivity (Scheme 38). This electrolyte- and base-free protocol exhibited broad substrate scope, accommodating both terminal and internal alkynes with excellent functional group tolerance.

4.2 Construction of central chirality

4.2.1 *P-stereogenic chirality*

In 2022, Shi's group [37] first reported the Co/Salox-catalyzed enantioselective desymmetrizing C–H/N–H activation/annulation of phosphinamides (Scheme 39). This protocol, consisting of commercially available Co(II) salts, easily prepared chiral Salox ligand, manganese salts and base additives, accommodated a wide range of internal/terminal alkynes and allenes, providing *P*-

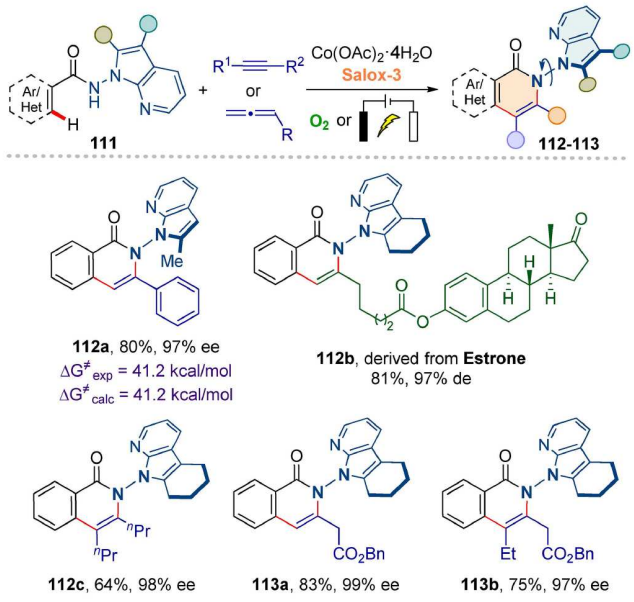

Scheme 37 (Color online) Co/Salox-enabled the atroposelective construction of the N–N axis.

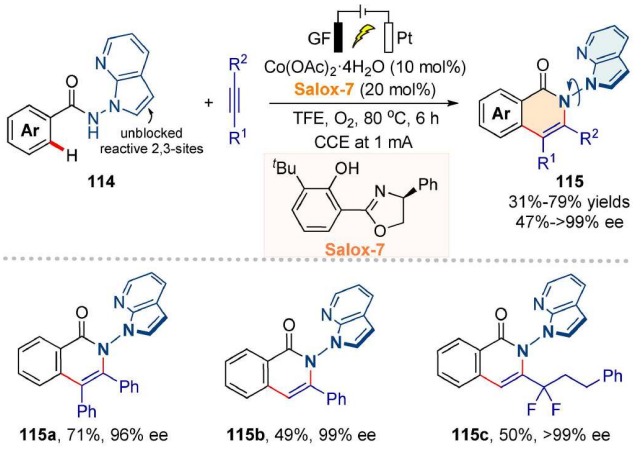

Scheme 38 (Color online) Cobaltaelectro-catalyzed atroposelective construction of N–N axis.

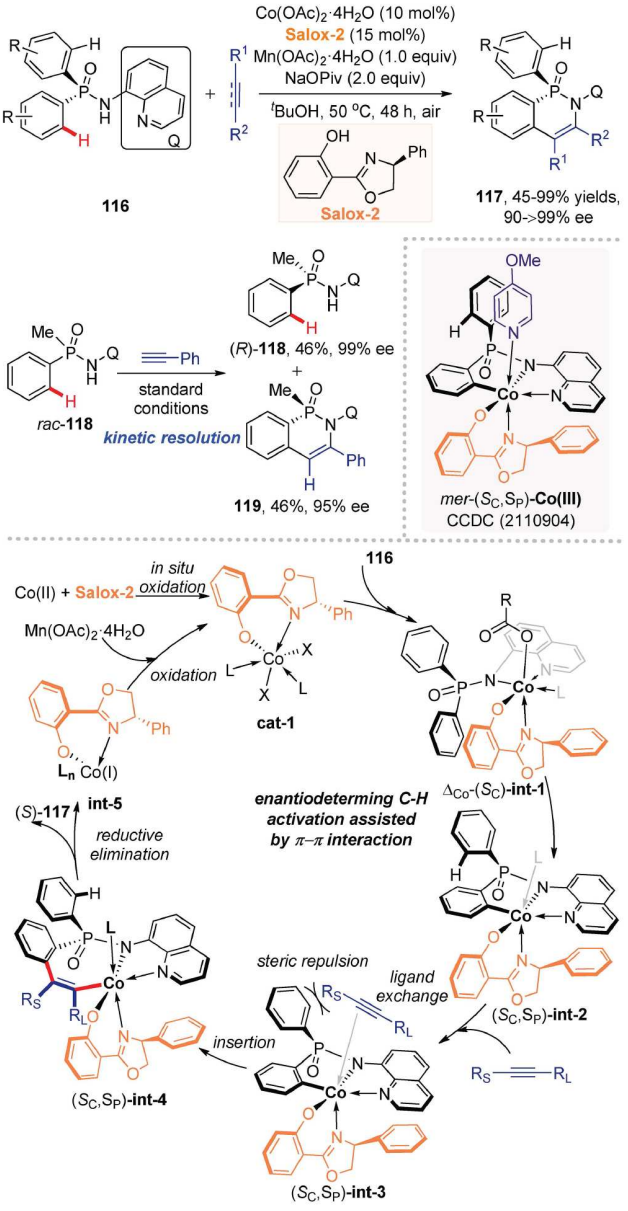

Scheme 39 (Color online) Co/Salox-catalyzed enantioselective desymmetrizing C–H activation of phosphinamides.

stereogenic compounds in high yield and excellent enantioselectivities. Beyond the desymmetrization reaction, the kinetic resolution of *rac*-**118** proceeded efficiently, delivering annulation product (46% yield 95% ee) and enabling the recovery of (*R*)-**118** (46% yield 99% ee) (*s* factor = 205.8). To probe the mechanism, substrate **116** was treated with 1 equiv $Co(OAc)_2·4H_2O$ and **Salox-2** in the presence of $Mn(OAc)_2·4H_2O$ oxidant, yielding octahedral cobaltacycle *mer*-(S_C,S_P)-**Co(III)** complex as a single diastereomer. This intermediate could be readily converted to the annulation product (99% ee), with its configuration matching the *P*-center in *mer*-(S_C, S_P)-**Co(III)** complex, indicating that the *P*-stereogenic chirality was established through enantiodetermining C–H cleavage. The reaction proceeded through (1) *in situ* oxidation of Co(II) salt, (2) precise assembly of substrate **116** with Salox ligand, (3) enantiodetermining C–H activation, (4) ligand exchange with alkynes followed by migratory insertion, (5) reductive elimination. Notably, π-π stacking interactions between the phenyl group of **Salox-2** and the AQ group of **116**, as well as between one phenyl ring of **116** and the phenolate group of **Salox-2** in **int-1**, are essential for high enantiocontrol.

Subsequently, Ling's group [120] achieved the construction of *P*-stereogenic chirality via electrochemically enabled cobalt-catalyzed enantioselective C–H annulation (Scheme 40). The reaction proceeded efficiently in a shorter time, avoiding the use of metal oxidants, compared to Shi's above work [37]. A broad range of internal/terminal alkynes, internal diynes, and alkynes containing drug fragments were well tolerated, delivering *P*-chiral cyclicphosphorus oxides with good yields and excellent enantioselectivities.

Ackermann's group [121] developed a cobaltaelectro-catalyzed enantioselective C–H annulation of allenes with phosphinic amides and benzamides (Scheme 41). This method efficiently produced a broad range of *P*-stereogenic and C–N axially chiral compounds in good yields with excellent enantiopurity. Moreover, decagram-scale reactions in continuous flow highlighted the synthetic potential of this enantioselective electrocatalysis approach.

Inspired by the high performance of Co/Salox catalysis, Shi's group [122] disclosed the enantioselective dehydrogenative C–H alkoxylation and amination of diarylphosphinamides, providing access to diverse *P*-stereogenic compounds (Scheme 42). In the C–H alkoxylation, dialkoxylated products were obtained in the presence

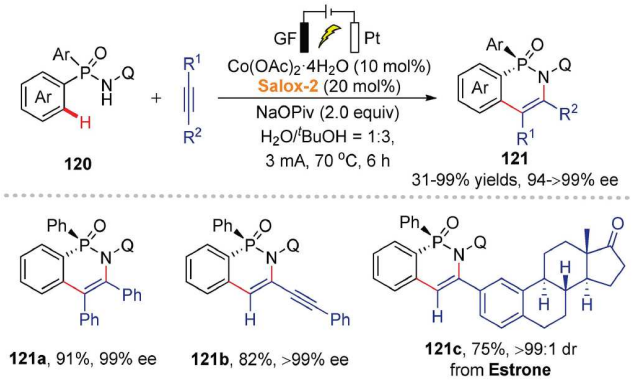

Scheme 40 (Color online) Cobaltaelectro-catalyzed enantioselective C–H annulation.

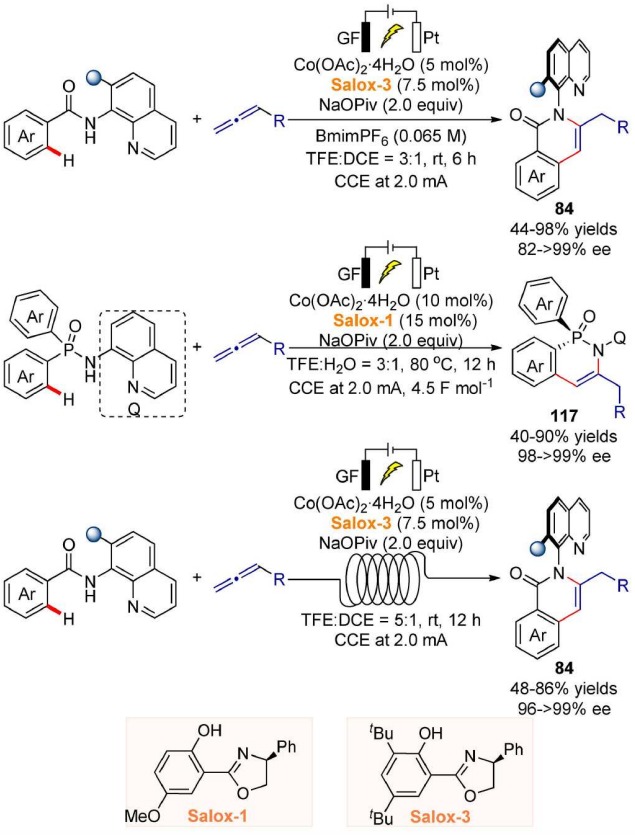

Scheme 41 (Color online) Cobaltaelectro-catalyzed enantioselective C–H annulation with allenes.

of 3 equivalents of Ag_2CO_3. Mechanistic studies revealed that Ag_2CO_3 oxidizes the octahedral Co(III) complex to Co(IV), followed by reductive elimination to afford the dimethoxylated product. This suggests a Co(III/IV/II) catalytic cycle, distinct from previous Co/Salox-catalyzed C–H activations. The resulting *P*-stereogenic phosphinamides could be further derivatized to both mono- and diphosphine chiral ligands. Additionally, Co/Salox-catalyzed dehydrogenative C–H amination with cyclic secondary amines was achieved under slightly modified conditions by replacing the Ag salt with $Mn(OAc)_3·2H_2O$ as the oxidant.

Shortly thereafter, the same group reported an electrochemical Co/Salox-catalyzed enantioselective C–H alkoxylation, replacing stoichiometric silver salts with electricity while generating H_2 as the sole byproduct [123] (Scheme 43). Mechanistic studies confirmed a Co(III/IV/II) catalytic cycle, wherein the Co(III) intermediate was oxidized to Co(IV) at the anode, a process facilitated by the base of

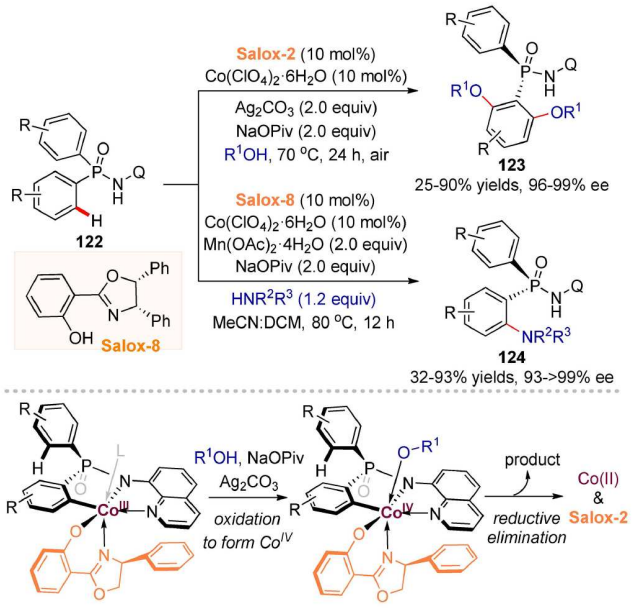

Scheme 42 (Color online) Co/Salox-catalyzed enantioselective C–H alkoxylation and amination.

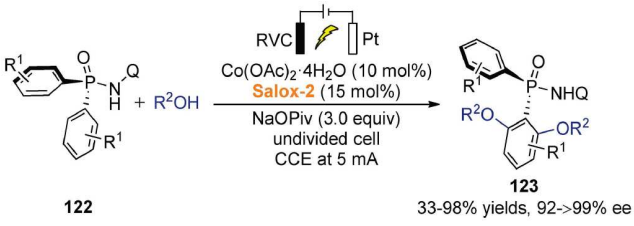

Scheme 43 (Color online) Cobaltaelectro-catalyzed enantioselective C–H alkoxylation.

NaOPiv.

Using the simple Co(II)/Salox catalysis, Sundararaju's group [124] reported an unconventional protocol for the regio-reversed, enantioselective C–H annulation of phosphinamides with bromoalkynes via desymmetrization (Scheme 44). The authors proposed that the reaction proceeded through (1) enantio-determining C–H activation, (2) regioselective bromoalkyne insertion into the Co–C bond, (3) reductive elimination, (4) oxidative addition of cobalt(I) species with C-Br followed by ligand exchange with pivalic acid, and (5) reductive elimination, yielding *P*-stereogenic compounds with excellent enantioselectivity.

In 2024, Ling's group [125] disclosed a Co/Salox-catalyzed enantioselective electrochemical C–H acyloxylation (Scheme 45). A broad range of *P*-stereogenic compounds was obtained with acceptable yields and high enantioselectivities. Moreover, the acyloxyl group is readily removable, providing *P*-chiral phosphamides with a free hydroxyl group.

Recently, Miao, Xu, and coworkers [126] disclosed a Co/Salox-catalyzed C–H activation/annulation of diarylphosphinamides with maleimide, for synthesizing *P*-stereogenic and C–N axially chiral cyclic phosphinamide derivatives (Scheme 46). DFT calculations revealed that *P*-chirality is established during C–H activation. For the C–N axial chirality, stepwise oxidation of two hydrogen atoms by Ag_2O occurs after the cyclization process, thus resulting in the formation of dual-chiral frameworks.

4.2.2 *C-stereogenic chirality*

Inspired by advances in the construction of axially chiral and

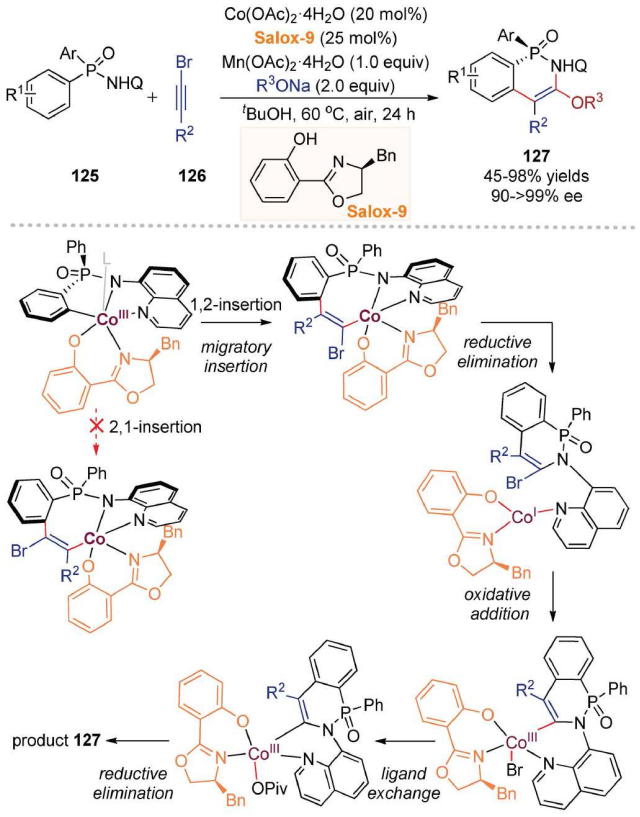

Scheme 44 (Color online) Co/Salox-catalyzed regio-reversed enantioselective C–H annulation.

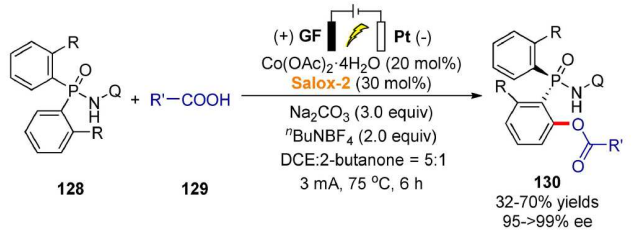

Scheme 45 (Color online) Cobaltaelectro-catalyzed asymmetric C–H acyloxylation.

P-stereogenic frameworks catalyzed by a simple Co/Salox system, our group explored its application in assembling *C*-stereogenic chirality. Using a naphthol-based chiral Salox ligand, we developed a cobalt-catalyzed C–H/N–H activation/annulation of benzamides with alkenes to synthesize chiral dihydroisoquinolone derivatives [127] (Scheme 47). The reaction typically proceeded efficiently within just 10–30 min. A broad range of terminal, internal, and cyclic alkenes was well tolerated, with cyclic alkenes exhibiting a notably opposite stereogenic configuration compared to terminal alkenes. Aliphatic α-olefins afforded a mixture of regioisomers in high yield and enantioselectivity. Moreover, the quinoline auxiliary could be smoothly removed to furnish dihydroisoquinolone in 60% yield without loss of enantiopurity, underscoring the practicability of this protocol.

Merging electrosynthesis with cobalt-catalyzed C–H activation offers a sustainable alternative, using electrons as clean redox reagents and avoiding the use of stoichiometric metal oxidants. In 2018, Lei's group [104] reported an achiral cobalt-catalyzed electrooxidative C–H annulation with olefins under divided-cell conditions to synthesize dihydroisoquinolones. In 2023, Shi's group developed the Co/Salox-catalyzed enantioselective electrooxidative

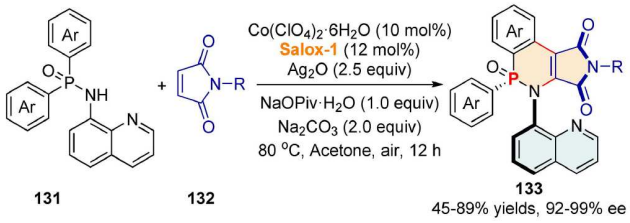

Scheme 46 (Color online) Co/Salox-enabled the *P*-stereogenic and C–N axially chiral phosphinamides.

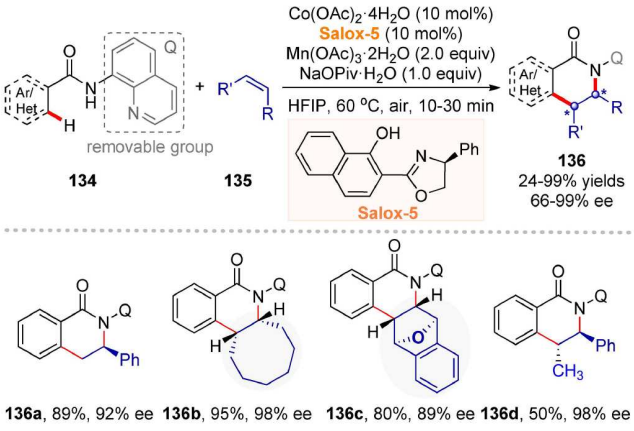

Scheme 47 (Color online) Co/Salox-enabled the construction of *C*-stereogenic frameworks.

C–H annulation of benzamides with olefins in an undivided cell [128] (Scheme 48). A broad range of styrenes, as well as aliphatic terminal olefins, were compatible with this protocol, delivering chiral dihydroisoquinolone in good yields, high regioselectivity, and excellent enantiopurity. The use of Salox ligand bearing a bulky *tert*-butyl group at the *ortho*-position of phenol and the addition of 3,4,5-trichloropyridine were crucial to the high level of regio- and enantiocontrol.

In 2024, Ackermann's group [129] developed a cobalt electrocatalyzed C–H annulation with alkenes for the construction of both central and axial chiralities with a high level of enantioselectivity and diastereoselectivity (Scheme 49). This electrocatalytic strategy enabled C–H/N–H activations and annulations with both cyclic and acyclic alkenes, providing efficient access to diverse centrally and axially chiral dihydroisoquinolinones while simultaneously generating hydrogen as a valuable byproduct. Investigations of the atropostability of the products revealed that the exceptionally mild reaction conditions afforded by the electrocatalytic system were crucial for achieving high stereoselectivities.

Shi's group [130] reported a highly enantioselective synthesis of chiral diarylmethylamines (DAMAs) via cobalt-catalyzed C–H alkoxylation of picolinamides by using a Co/Salox catalysis (Scheme 50). Through desymmetrization, a variety of chiral DAMAs were obtained in high yields (up to 90%) with excellent enantioselectivity (up to 99% ee). Additionally, the protocol enables the synthesis of chiral benzylamines via kinetic resolution.

The same group also developed a C–H/N–H activation/annulation of picolinamides with alkynes, affording C_1-chiral 1,2-dihydroisoquinolines (DHIQs) in good yields and high enantiopurities [131] (Scheme 51). This protocol enabled the asymmetric synthesis of several tetrahydroisoquinoline alkaloids, including (*S*)-norlaudanosine, (*S*)-sebiferine, (*S*)-xylopinine, as well as key intermediates of (+)-solifenacin, FR115427, and (+)-NPS R-568.

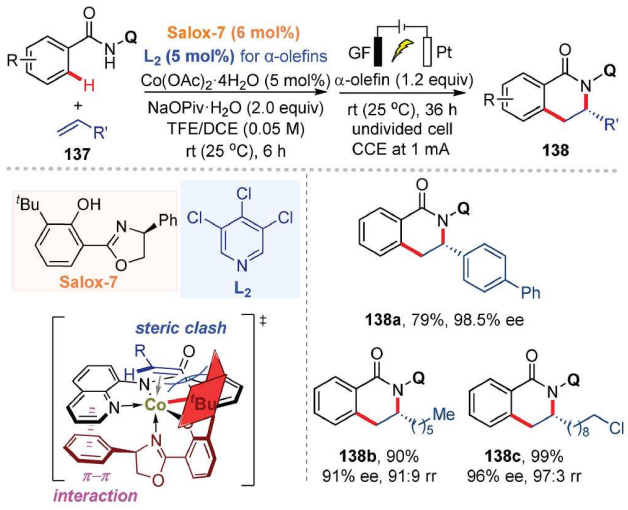

Scheme 48 (Color online) Electrochemical cobalt-catalyzed enantioselective C–H/N–H annulation with alkenes.

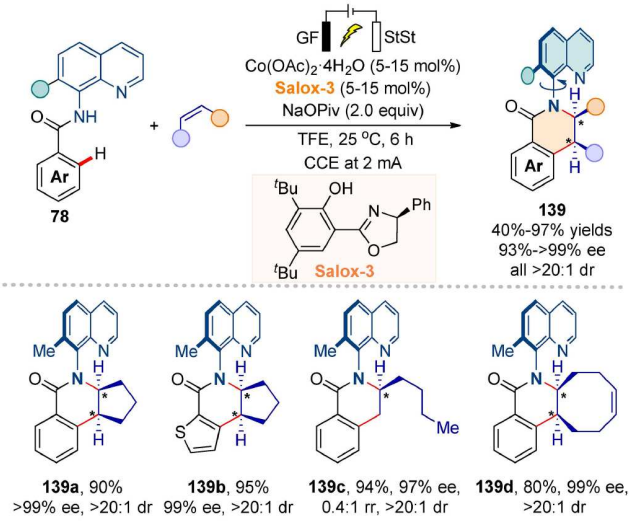

Scheme 49 (Color online) Electrochemical cobalt-catalyzed enantioselective C–H/N–H annulation with alkenes.

Scheme 50 (Color online) Cobalt-catalyzed C–H alkoxylation to access DAMAs.

In 2024, Shi, Yao, and coworkers [132] disclosed a Co/Salox-catalyzed enantioselective domino [3 + 2] annulation with symmetrical bicyclic alkenes for the synthesis of chiral bridged bicycles (Scheme 52). Notably, Cheng's group [133] had previously explored the possibility of diastereoselective [3 + 2] annulation catalyzed by inexpensive cobalt(II) salts in a racemic version in 2016. In their study, the *in situ*-removed AQ was found to inhibit catalytic activity by coordinating with the cobalt catalyst. To address this issue, Shi's group [130] employed 2-methylbutyraldehyde as a trapping agent for AQ, forming an imine that

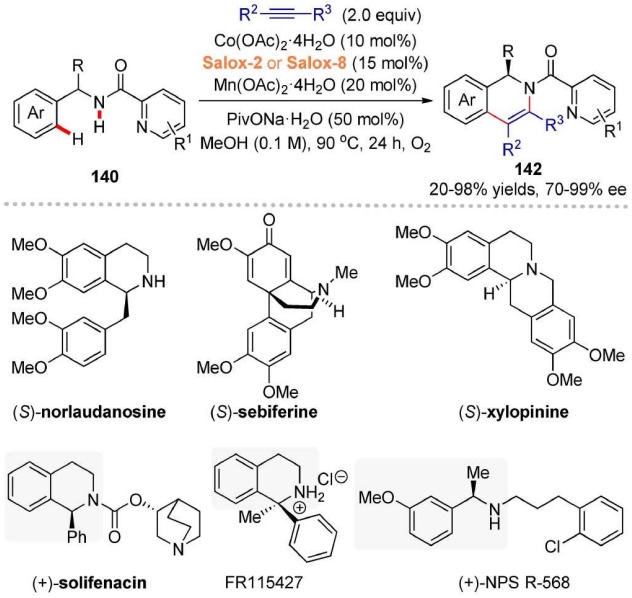

Scheme 51 (Color online) Cobalt-catalyzed C–H annulation to access DHIQs.

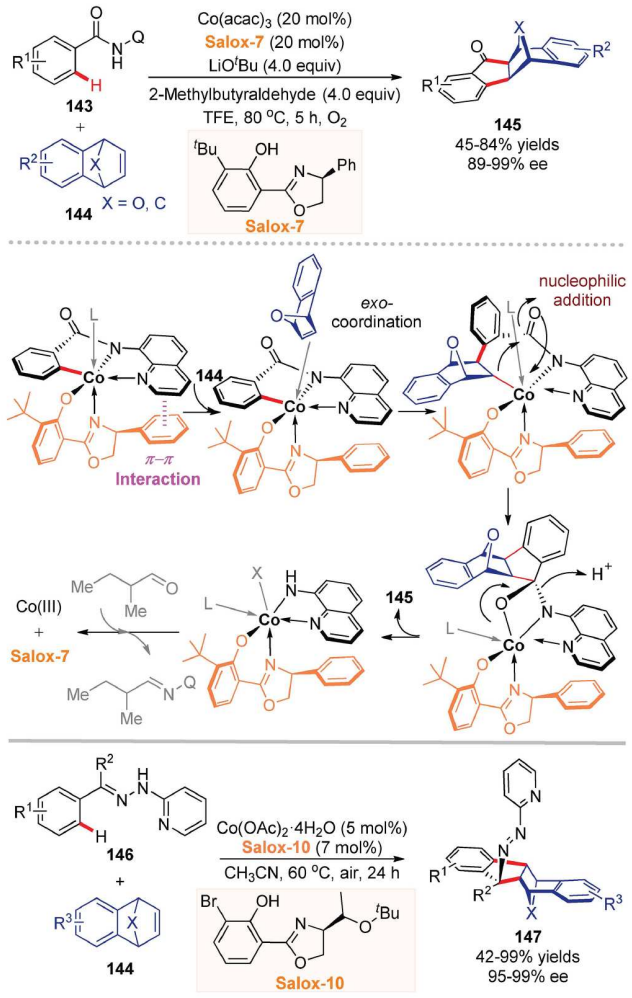

Scheme 52 (Color online) Co/Salox-catalyzed enantioselective domino [3 + 2] annulation.

subsequently liberated the cobalt catalyst and the Salox ligand, thereby enabling the catalytic cycle to proceed. Mechanistic studies further revealed that the addition of *t*-BuOLi not only facilitated the

release of the Salox ligand but also promoted the C–H activation step. The reaction proceeded via (1) enantioselective C–H insertion, (2) nucleophilic addition procedure (rather than C–N reductive elimination or β-oxygen elimination), (3) C–N bond cleavage, (4) release of trivalent cobalt and the Salox ligand. Moreover, the authors extended this strategy for the synthesis of chiral bridged bicycles based on indane derivatives by using a newly designed Salox ligand, building upon earlier racemic work reported by Volla's group [134]. Worthy of note, Shi's group [135] recently achieved the typical [4 + 2] annulation of benzamide with oxabicyclic alkenes enabled by a Ni/Salox catalysis, further demonstrating the robustness and broad applicability of Salox ligands in 3d transition-metal-catalyzed enantioselective C–H activations.

Recently, Ackermann's group [136] developed the cobalt- or nickel-catalyzed distinctive enantioselective C–H annulations under electrochemical conditions (Scheme 53). Both electrocatalytic systems delivered high enantio- and diastereoselectivity, directly generating versatile chiral building blocks with multiple stereocenters. Mechanistic investigations by experimental and computational studies reveal cobalt(III) proceeds through C–C nucleophilic addition while nickel(III) undergoes C–N reductive elimination as product-determining steps. Moreover, the same group disclosed a cobaltaelectro-catalyzed C–H activation/annulation to access chiral indane derivatives, by using a κ^2-*N*,*O*-oxazoline ligands [137]. They employed DFT-derived descriptors and regression modeling to parameterize chiral κ^2-*N*,*O*-oxazoline preligand modularity, developing a selectivity model based on key steric, electronic, and interaction parameters.

Almost at the same time, Shi's [138], Zhang's [139], Sundararaju's [140], and Ackermann's [141] groups independently developed dual cobalt-photoredox catalytic systems for the C–H activation/annulation of benzamides with *N*-pyrimidyl indoles (Scheme 54). These transformations efficiently generated a broad range of chiral indoline derivatives, demonstrating the potential of photoinduced cobalt catalysis for enantioselective C–H functionalization. Notably, Ackermann's group [141] further demonstrated the system's robustness by achieving enantioselective annulations with alkenes, allenes, and alkynes under continuous photoflow conditions, enabling construction of both central and axial chiralities.

4.3 Construction of inherent chirality

Inherent chirality represents a unique class of chiral entities distinct from conventional chiral molecules exhibiting central, axial, planar, or helical chirality. However, the catalytic asymmetric synthesis of inherently chiral frameworks remains underdeveloped. Among these, calix[4]arenes have attracted significant attention due to their distinctive structural features and broad potential applications in asymmetric catalysis, chiral recognition, and related fields. Leveraging advances in cobalt-catalyzed C–H activation/functionalization, several sophisticated strategies have recently emerged for constructing inherently chiral calix[4]arenes.

In 2024, our group achieved the simultaneous construction of axial and inherent chirality through cobalt-catalyzed asymmetric C–H activation/annulation using O_2 as the oxidant [142] (Scheme 55). This one-step protocol is compatible with various calix[4]-arenes and alkynes, affording inherently chiral calix[4]arenes bearing a chiral C–N axis in high yields (up to 94%) with excellent diastereo- (up to 95%) and enantioselectivity (up to 95%). The chiral recognition ability and circularly polarized luminescence (CPL) properties of these products highlight their potential applications.

Meanwhile, Shi's group [143] reported a similar approach for

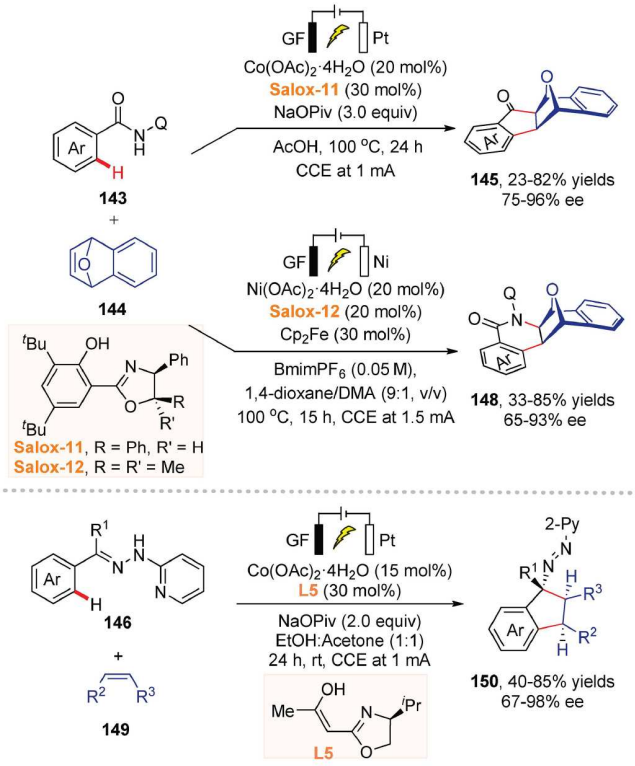

Scheme 53 (Color online) Electrochemical cobalt or nickel-catalyzed enantioselective C–H activations.

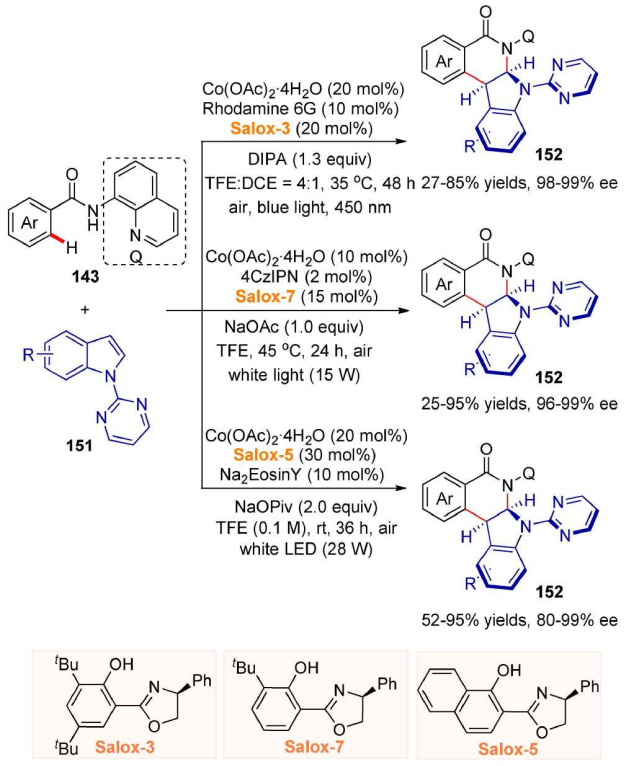

Scheme 54 (Color online) Enantioselective cobaltaphotoredox-catalyzed C–H activation.

constructing inherently chiral calix[4]arenes with axial chirality through cobalt-catalyzed asymmetric C–H activation/annulation from prochiral calix[4]arenes and alkynes, employing 8-aminoquinoline as the directing group (Scheme 56). In contrast to our method, their transformation could utilize either Mn(III) oxidants or

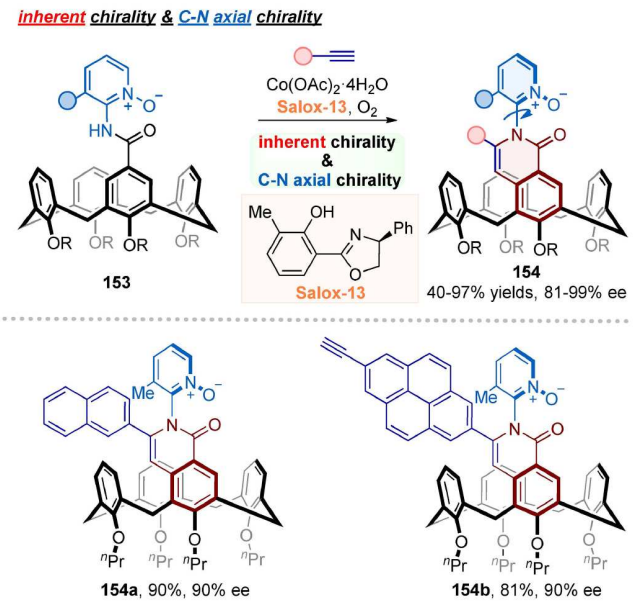

Scheme 55 (Color online) Co/Salox-catalyzed asymmetric construction of both inherent and axial chirality.

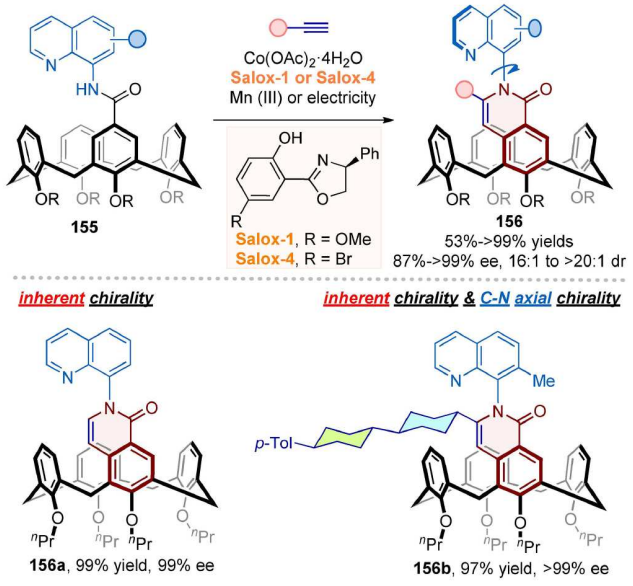

Scheme 56 (Color online) Co/Salox-catalyzed asymmetric construction of inherent, both inherent and axial chirality.

electrooxidation. Notably, when using acetylene, the reaction produced inherently chiral calix[4]arenes in up to 99% yield and 99% ee. The incorporation of substituted terminal alkynes similarly afforded calix[4]arenes bearing both inherent and axial chirality with excellent yields and enantioselectivities. The resulting products exhibited intriguing fluorescence properties, demonstrating promising potential for optoelectronic applications.

Recently, our group developed an enantioselective electrosynthesis of inherently chiral calix[4]arenes via cobalt-catalyzed asymmetric C–H acyloxylation using pyridine *N*-oxide as the directing group [144] (Scheme 57). Starting from prochiral macrocyclic precursors, this transformation exhibits broad substrate scope and good functional group tolerance, accommodating diverse carboxylic acids, including primary, secondary, tertiary aliphatic, and aryl variants. The method delivers acyloxylated inherently chiral calix-

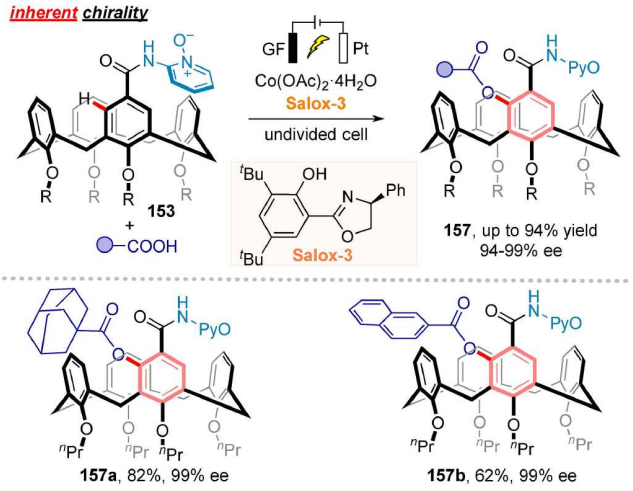

Scheme 57 (Color online) Co/Salox-catalyzed asymmetric C–H acyloxylation to construct inherent chirality.

[4]arenes in up to 94% isolated yield and 99% ee.

4.4 Construction of planar chirality

The asymmetric synthesis of planar chiral molecules remains a significant challenge, with only limited established strategies—primarily intramolecular asymmetric annulation and catalytic desymmetrization through stereoselective functionalization. Among metallocene-based planar chiral scaffolds, ferrocenes have emerged as privileged frameworks with wide applications in asymmetric catalysis, pharmaceutical development, and materials science. A significant breakthrough was achieved by Shi and Yao, who developed a cobalt-catalyzed asymmetric synthesis of oxygen-substituted planar chiral ferrocenes via C–H activation/acyloxylation [145] (Scheme 58). The key to this transformation lies in a dual-ligand system comprising a chiral salicycloazoline ligand and a phosphine oxide ligand, which enables excellent enantioselectivity (up to 99% ee) and good yields (up to 83%) across a broad range of substrates, including both aromatic and aliphatic carboxylic acids. Through comprehensive mechanistic studies incorporating control experiments, deuterium-labelling studies, and kinetic isotope effect measurements, the authors identified a crucial chiral octahedral cobalt(III) intermediate. This intermediate is stabilized through coordination with the neutral phosphine oxide ligand, providing important insights into the reaction pathway.

Given the broad utility of chiral [22]paracyclophanes (PCPs) in asymmetric catalysis and materials science, Shi's group [146] recently reported a cobalt/Salox-catalyzed enantioselective C–H acyloxylation/alkoxylation of racemic PCPs using carboxylic acids or alcohols under electrooxidative or photoredox conditions (Scheme 59). This method employs electrons or O_2 instead of stoichiometric metal oxidants, enabling the mild and efficient synthesis of oxygenated PCPs with up to 50% yield (99% ee) and recovering the unreacted enantiomer (49% yield, 99% ee), achieving remarkable *s*-factors of up to 1057.

Very recently, Ackermann's group [147] developed a cobalta-photoredox dual catalysis for the construction of central and planar chiral [22]paracyclophane derivatives through kinetic resolution (Scheme 60). This approach affords diverse multi-chiral PCPs in good yields with excellent stereocontrol (>20:1 dr, >99% ee), while simultaneously recovering the unreacted enantiomer with high enantiopurity (up to 50% yield, >99% ee). DFT calculations elucidated the enantioselectivity origin, showing a 5.2 kcal/mol

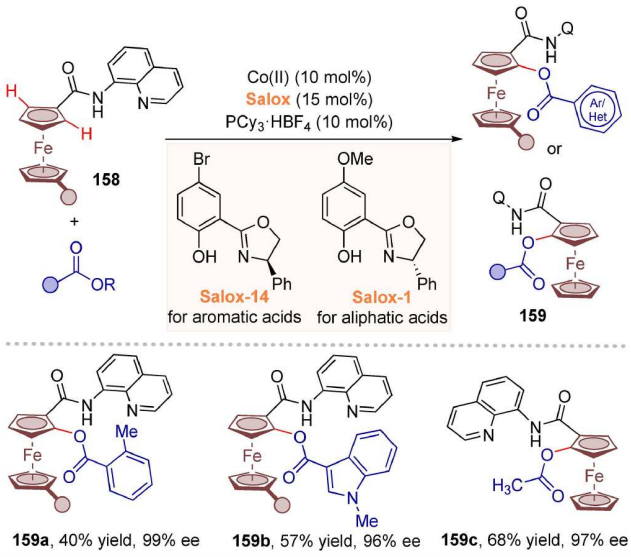

Scheme 58 (Color online) Cobalt/Salox-catalyzed asymmetric synthesis of oxygen-substituted planar chiral ferrocenes.

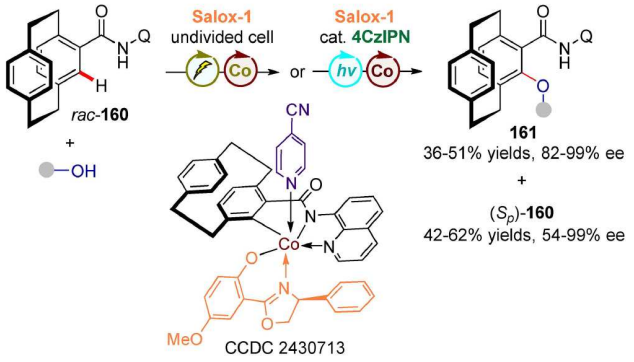

Scheme 59 (Color online) Cobalt/Salox-catalyzed asymmetric electrooxidative or photoredox C–H activation to access chiral PCPs.

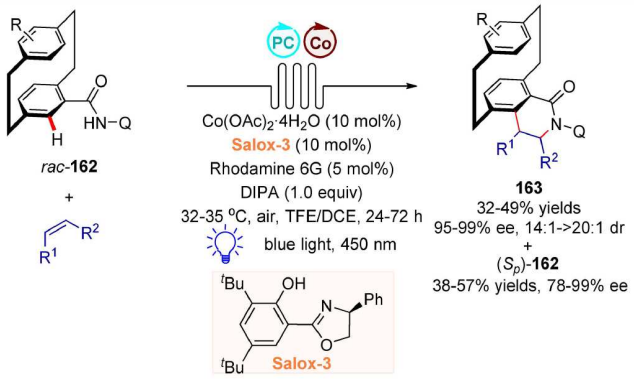

Scheme 60 (Color online) Cobaltaphotoredox catalysis for the construction of multi-chiral PCPs.

lower barrier for R_p *versus* S_p during alkene migratory insertion. Moreover, gram-scale continuous photoflow synthesis and versatile transformations of the products further highlight the synthetic utility of the protocol.

5 Summary and outlook

Cobalt-catalyzed enantioselective C–H functionalization has achieved significant progress, offering a sustainable and efficient approach to constructing chiral molecules. Three different catalytic models have been established based on the involvement of key intermediates and mechanistic pathways: (1) low-valent Co(I) catalysis, (2) Cp*Co(III)/CCA, and Cp^{x}Co(III) catalysis, and (3) *in situ*-oxidized Co(III)/Salox system.

In low-valent Co(I) catalysis, commercially available cobalt salts are reduced to active Co(I) species, which facilitate C–H bond activation through insertion to form a key Co(III)-H intermediate. Subsequent stereoselective C–H functionalization is mediated by chiral phosphine or *N*-heterocyclic carbene (NHC) ligands. While this approach has proven particularly effective for activated C–H bonds (including acyl, allylic, and electron-rich heteroarenes), its extension to unactivated aryl and aliphatic C–H systems presents a significant yet promising challenge for future research. Further development of catalytic reductant systems, as opposed to the current stoichiometric requirements, could substantially expand both substrate scope and process sustainability. Moreover, while existing transformations primarily rely on Co-H additions to unsaturated bonds, developing alternative activation mechanisms might significantly expand the structural diversity of chiral products.

The high-valent cyclopentadienyl (Cp) cobalt catalytic system has demonstrated remarkable potential in asymmetric C–H functionalizations. Assisted by a suitable monodentate directing group, achiral Cp*Co(III) catalyst in combination with chiral carboxylic acid (CCA) ligands, typically derived from protected amino acids or axially/spiro-chiral frameworks, has been applied for both sp^2 and sp^3 C–H bonds asymmetric functionalization. Notably, the design of chiral cyclopentadienyl (Cp^x) ligands based on binaphthyl frameworks, along with their corresponding cobalt catalysts, has enabled diverse transformations, including C–H annulation and multi-component alkylations. These advances highlight cobalt's unique reactivity and selectivity compared to noble rhodium and iridium metals, solidifying its promise as an earth-abundant alternative for asymmetric catalysis. While significant progress has been made, further opportunities exist to deepen the understanding and expand the scope of this field. The origin of stereocontrol induced by chiral carboxylic acids requires deeper elucidation, while establishing fundamental principles for ligand design would significantly advance future catalyst development. On the other hand, although binaphthyl-based chiral Cp^x ligands have demonstrated remarkable efficacy, the development of structurally diverse ligand scaffolds—especially those featuring streamlined synthetic routes—would substantially expand the applicability of chiral Cp^{x}Co(III) systems. Furthermore, expanding comparative studies on Cp* *versus* tailored Cp^x ligands, along with parallel evaluations of Cp^{x}Co *versus* Cp^{x}Rh complexes, may elucidate the fundamental relationship of structure with regio-/enantioselectivity, thus providing a blueprint for catalytic system design.

The Co(III)/Salox system, facilitated by a bidentate directing group, has recently emerged as a cost-effective and versatile platform for asymmetric C–H activation. This approach enables facile construction of diverse stereogenic elements, including axial, central, planar, and inherent chirality, as well as multiple chiral architectures. The catalytically active Co(III) species is generated *in situ* through oxidation of inexpensive Co(II) salts using various methods, including O_2 atmosphere, manganese/silver additives, or electrochemical/photoredox conditions, thereby eliminating the requirement for *pre*-synthesized Co(III) complexes. Notably, the isolation of key octahedral Co(III) intermediates, in combination with DFT computational studies, has provided mechanistic clarity regarding both catalytic cycle progress and enantiocontrol origin. In the future, the extension of this strategy to more challenging

unactivated sp^3 C–H bond functionalization would represent a significant breakthrough in asymmetric catalysis. While current systems still require the preinstallation of bidentate directing groups to stabilize the key octahedral cobalt intermediates, future efforts could focus on developing direct and atom-economical C–H functionalization methods that enable efficient construction of valuable chiral scaffolds. A particularly promising direction involves exploring applications of these new architectures in the area of advanced materials science and pharmaceutical chemistry.

We believe that this field holds tremendous potential for transformative development in the coming years, where significant breakthroughs in earth-abundant cobalt-catalyzed asymmetric C–H functionalization will enable efficient construction of diverse chiral molecules.

Conflict of interest

The authors declare no conflict of interest.

Acknowledgement

This work was supported by the National Natural Science Foundation of China (22271260 to Jun-Long Niu) and the Natural Science Foundation of Henan Province (232301420007, 242300421033 to Jun-Long Niu; 242301420059, 252300421178 to Dandan Yang).

References

1 Wencel-Delord J, Glorius F. *Nat Chem*, 2013, 5: 369–375
2 Baudoin O. *Angew Chem Int Ed*, 2020, 59: 17798–17809
3 Basu D, Kumar S, V SS, Bandichhor R. *J Chem Sci*, 2018, 130: 71
4 Yamaguchi J, Yamaguchi AD, Itami K. *Angew Chem Int Ed*, 2012, 51: 8960–9009
5 Newton CG, Wang SG, Oliveira CC, Cramer N. *Chem Rev*, 2017, 117: 8908–8976
6 Giri R, Shi BF, Engle KM, Maugel N, Yu JQ. *Chem Soc Rev*, 2009, 38: 3242–3272
7 Park Y, Kim Y, Chang S. *Chem Rev*, 2017, 117: 9247–9301
8 Achar TK, Maiti S, Jana S, Maiti D. *ACS Catal*, 2020, 10: 13748–13793
9 Liu CX, Yin SY, Zhao F, Yang H, Feng Z, Gu Q, You SL. *Chem Rev*, 2023, 123: 10079–10134
10 Zhan BB, Jin L, Shi BF. *Trends Chem*, 2022, 4: 220–235
11 Shao Q, Wu K, Zhuang Z, Qian S, Yu JQ. *Acc Chem Res*, 2020, 53: 833–851
12 Yoshino T, Matsunaga S. *ACS Catal*, 2021, 11: 6455–6466
13 Yoshino T, Satake S, Matsunaga S. *Chem Eur J*, 2020, 26: 7346–7357
14 Loup J, Dhawa U, Pesciaioli F, Wencel-Delord J, Ackermann L. *Angew Chem Int Ed*, 2019, 58: 12803–12818
15 Choppin S, Wencel-Delord J. *Acc Chem Res*, 2023, 56: 189–202
16 Li LJ, He Y, Yang Y, Guo J, Lu Z, Wang C, Zhu S, Zhu SF. *CCS Chem*, 2024, 6: 537–584
17 Woźniak Ł, Cramer N. *Trends Chem*, 2019, 1: 471–484
18 Li JF, Luan YX, Ye M. *Sci China Chem*, 2021, 64: 1923–1937
19 Gao K, Yoshikai N. *Acc Chem Res*, 2014, 47: 1208–1219
20 Baccalini A, Vergura S, Dolui P, Zanoni G, Maiti D. *Org Biomol Chem*, 2019, 17: 10119–10141
21 Xu W, Ye M. *Synthesis*, 2022, 54: 4773–4783
22 Zheng Y, Zheng C, Gu Q, You SL. *Chem Catal*, 2022, 2: 2965–2985
23 Garai B, Das A, Kumar DV, Sundararaju B. *Chem Commun*, 2024, 60: 3354–3369
24 Yao QJ, Shi BF. *Acc Chem Res*, 2025, 58: 971–990
25 Murahashi S. *J Am Chem Soc*, 1955, 77: 6403–6404
26 Gao K, Lee PS, Fujita T, Yoshikai N. *J Am Chem Soc*, 2010, 132: 12249–12251
27 Yoshino T, Ikemoto H, Matsunaga S, Kanai M. *Angew Chem Int Ed*, 2013, 52: 2207–2211
28 Grigorjeva L, Daugulis O. *Angew Chem Int Ed*, 2014, 53: 10209–10212
29 Sauermann N, Meyer TH, Tian C, Ackermann L. *J Am Chem Soc*, 2017, 139: 18452–18455
30 Gao X, Wang P, Zeng L, Tang S, Lei A. *J Am Chem Soc*, 2018, 140: 4195–4199
31 Dwivedi V, Kalsi D, Sundararaju B. *ChemCatChem*, 2019, 11: 5160–5187
32 Yang J, Yoshikai N. *J Am Chem Soc*, 2014, 136: 16748–16751
33 Pesciaioli F, Dhawa U, Oliveira JCA, Yin R, John M, Ackermann L. *Angew Chem Int Ed*, 2018, 57: 15425–15429
34 Fukagawa S, Kato Y, Tanaka R, Kojima M, Yoshino T, Matsunaga S. *Angew Chem Int Ed*, 2019, 58: 1153–1157
35 Ozols K, Jang YS, Cramer N. *J Am Chem Soc*, 2019, 141: 5675–5680
36 Si XJ, Yang D, Sun MC, Wei D, Song MP, Niu JL. *Nat Synth*, 2022, 1: 709–718
37 Yao Q, Chen J, Song H, Huang F, Shi B. *Angew Chem Int Ed*, 2022, 61: e202202892
38 Hu Y, Lang K, Li C, Gill JB, Kim I, Lu H, Fields KB, Marshall MK, Cheng Q, Cui X, Wojtas L, Zhang XP. *J Am Chem Soc*, 2019, 141: 18160–18169
39 Moselage M, Li J, Ackermann L. *ACS Catal*, 2016, 6: 498–525
40 Oliveira JCA, Dhawa U, Ackermann L. *ACS Catal*, 2021, 11: 1505–1515
41 Whyte A, Torelli A, Mirabi B, Prieto L, Rodríguez JF, Lautens M. *J Am Chem Soc*, 2020, 142: 9510–9517
42 Whyte A, Bajohr J, Torelli A, Lautens M. *Angew Chem Int Ed*, 2020, 59: 16409–16413
43 Murphy SK, Dong VM. *Chem Commun*, 2014, 50: 13645–13649
44 Yang J, Rérat A, Lim YJ, Gosmini C, Yoshikai N. *Angew Chem Int Ed*, 2017, 56: 2449–2453
45 Kim DK, Riedel J, Kim RS, Dong VM. *J Am Chem Soc*, 2017, 139: 10208–10211
46 Park JW, Kou KGM, Kim DK, Dong VM. *Chem Sci*, 2015, 6: 4479–4483
47 Park JW, Chen Z, Dong VM. *J Am Chem Soc*, 2016, 138: 3310–3313
48 Liu JB, Wang Y, Wang HY, Liu XJ. *Org Chem Front*, 2025, 12: 2194–2204
49 Santhoshkumar R, Mannathan S, Cheng CH. *J Am Chem Soc*, 2015, 137: 16116–16120
50 Lee PS, Yoshikai N. *Org Lett*, 2015, 17: 22–25
51 Jacob N, Zaid Y, Oliveira JCA, Ackermann L, Wencel-Delord J. *J Am Chem Soc*, 2022, 144: 798–806
52 Gao K, Yoshikai N. *J Am Chem Soc*, 2011, 133: 400–402
53 Luc A, Oliveira JCA, Boos P, Jacob N, Ackermann L, Wencel-Delord J. *Chem Catal*, 2023, 3: 100765
54 Kazerouni AM, McKoy QA, Blakey SB. *Chem Commun*, 2020, 56: 13287–13300
55 Mita T, Hanagata S, Michigami K, Sato Y. *Org Lett*, 2017, 19: 5876–5879
56 Zhang H, Huang J, Meng F. *Cell Rep Phys Sci*, 2021, 2: 100406
57 Lukasevics L, Cizikovs A, Grigorjeva L. *Chem Commun*, 2021, 57: 10827–10841
58 Chandra D, Manisha D, Sharma U. *Chem Record*, 2022, 22: e202100271
59 Zell D, Bursch M, Müller V, Grimme S, Ackermann L. *Angew Chem Int Ed*, 2017, 56: 10378–10382
60 Kurihara T, Kojima M, Yoshino T, Matsunaga S. *Asian J Org Chem*, 2020, 9: 368–371
61 Liu YH, Xie PP, Liu L, Fan J, Zhang ZZ, Hong X, Shi BF. *J Am Chem Soc*, 2021, 143: 19112–19120
62 Zhang ZJ, Li SW, Oliveira JCA, Li Y, Chen X, Zhang SQ, Xu LC, Rogge T, Hong X, Ackermann L. *Nat Commun*, 2023, 14: 3149
63 Tan PW, Mak AM, Sullivan MB, Dixon DJ, Seayad J. *Angew Chem Int Ed*, 2017, 56: 16550–16554
64 Sekine D, Ikeda K, Fukagawa S, Kojima M, Yoshino T, Matsunaga S. *Organometallics*, 2019, 38: 3921–3926
65 Staronova L, Yamazaki K, Xu X, Shi H, Bickelhaupt FM, Hamlin TA, Dixon DJ. *Angew Chem Int Ed*, 2024, 63: e202316021
66 Jia C, Lu W, Oyamada J, Kitamura T, Matsuda K, Irie M, Fujiwara Y. *J Am Chem Soc*, 2000, 122: 7252–7263
67 Jia C, Piao D, Oyamada J, Lu W, Kitamura T, Fujiwara Y. *Science*, 2000, 287: 1992–1995
68 Shi B, Maugel N, Zhang Y, Yu J. *Angew Chem Int Ed*, 2008, 47: 4882–4886
69 Liu YH, Li PX, Yao QJ, Zhang ZZ, Huang DY, Le MD, Song H, Liu L, Shi BF. *Org Lett*, 2019, 21: 1895–1899
70 Bentley R. *Chem Soc Rev*, 2005, 34: 609–624
71 Diesel J, Cramer N. *ACS Catal*, 2019, 9: 9164–9177
72 Hirata Y, Sekine D, Kato Y, Lin L, Kojima M, Yoshino T, Matsunaga S. *Angew Chem Int Ed*, 2022, 61: e202205341
73 Zhou YB, Zhou T, Qian PF, Li JY, Shi BF. *ACS Catal*, 2022, 12: 9806–9811
74 Murata A, Endo T, Hirata Y, Higashida K, Yoshino T, Matsunaga S. *Org Chem Front*, 2025, 12: 4236–4241
75 Ye B, Cramer N. *Acc Chem Res*, 2015, 48: 1308–1318
76 Newton CG, Kossler D, Cramer N. *J Am Chem Soc*, 2016, 138: 3935–3941
77 Hyster TK, Dalton DM, Rovis T. *Chem Sci*, 2015, 6: 254–258
78 Hyster TK, Dalton DM, Rovis T. *Chem Sci*, 2018, 9: 8024
79 Ozols K, Onodera S, Woźniak Ł, Cramer N. *Angew Chem Int Ed*, 2021, 60: 655–659
80 Lerchen A, Knecht T, Daniliuc CG, Glorius F. *Angew Chem Int Ed*, 2016, 55: 15166–15170
81 Shen Y, Liu G, Zhou Z, Lu X. *Org Lett*, 2013, 15: 3366–3369
82 Xing YY, Liu JB, Sun CZ, Huang F, Chen DZ. *Inorg Chem*, 2018, 57: 10726–10735
83 Boerth JA, Hummel JR, Ellman JA. *Angew Chem Int Ed*, 2016, 55: 12650–12654
84 Herraiz AG, Cramer N. *ACS Catal*, 2021, 11: 11938–11944
85 Zheng Y, Zhang WY, Gu Q, Zheng C, You SL. *Nat Commun*, 2023, 14: 1094
86 Muralirajan K, Prakash S, Cheng C. *Adv Synth Catal*, 2017, 359: 513–518
87 Zheng Y, Xie PP, Zheng C, You SL. *CCS Chem*, 2025, 7: 1202–1215
88 Verdhi LK, Wodrich MD, Cramer N. *J Am Chem Soc*, 2025, 147: 15041–15049
89 Shaaban S, Li H, Merten C, Antonchick AP, Waldmann H. *Synthesis*, 2021, 53: 2192–2200
90 Lukasevics L, Oh GN, Wang X, Grigorjeva L, Daugulis O. *J Am Chem Soc*, 2025, 147: 2476–2490
91 Yuan W, Shi B. *Angew Chem Int Ed*, 2021, 60: 23187–23192
92 Kitagawa O. *Acc Chem Res*, 2021, 54: 719–730
93 Zhang ZX, Zhai TY, Ye LW. *Chem Catal*, 2021, 1: 1378–1412
94 Mei GJ, Koay WL, Guan CY, Lu Y. *Chem*, 2022, 8: 1855–1893
95 Zilate B, Castrogiovanni A, Sparr C. *ACS Catal*, 2018, 8: 2981–2988
96 Wang YB, Tan B. *Acc Chem Res*, 2018, 51: 534–547
97 Wang F, Li X. *Chin J Org Chem*, 2022, 42: 4350–4352
98 Kikuchi J, Yoshikai N. *Nat Synth*, 2022, 1: 674–675

99 Li T, Shi L, Zhao X, Wang J, Si XJ, Yang D, Song MP, Niu JL. *Org Lett*, 2023, 25: 5191–5196
100 Wang X, Si XJ, Sun Y, Wei Z, Xu M, Yang D, Shi L, Song MP, Niu JL. *Org Lett*, 2023, 25: 6240–6245
101 Wang B, Xu G, Huang Z, Wu X, Hong X, Yao Q, Shi B. *Angew Chem Int Ed*, 2022, 61: e202208912
102 Zhang J, Liu X. *Chin J Org Chem*, 2022, 42: 3899
103 Ackermann L. *Acc Chem Res*, 2020, 53: 84–104
104 Tang S, Wang D, Liu Y, Zeng L, Lei A. *Nat Commun*, 2018, 9: 798
105 von Münchow T, Dana S, Xu Y, Yuan B, Ackermann L. *Science*, 2023, 379: 1036–1042
106 Si XJ, Zhao X, Wang J, Wang X, Zhang Y, Yang D, Song MP, Niu JL. *Chem Sci*, 2023, 14: 7291–7303
107 Hao XQ, Chen LJ, Ren B, Li LY, Yang XY, Gong JF, Niu JL, Song MP. *Org Lett*, 2014, 16: 1104–1107
108 Zhang L, Hao X, Liu Z, Zheng X, Zhang S, Niu J, Song M. *Angew Chem Int Ed*, 2015, 54: 10012–10015
109 Zhang L, Hao X, Zhang S, Liu Z, Zheng X, Gong J, Niu J, Song M. *Angew Chem Int Ed*, 2015, 54: 272–275
110 Zhang Y, Liu SL, Li T, Xu M, Wang Q, Yang D, Song MP, Niu JL. *ACS Catal*, 2024, 14: 1–9
111 Qian PF, Wu YX, Hu JH, Chen JH, Zhou T, Yao QJ, Zhang ZH, Wang BJ, Shi BF. *J Am Chem Soc*, 2025, 147: 10791–10802
112 Bei W, Pan J, Ran D, Liu Y, Yang Z, Feng R. *Chin J Org Chem*, 2023, 43: 3226–3238
113 Boos P, Pandit NK, Dana S, von Münchow T, Hashidoko A, Haberstock L, Herbst-Irmer R, Stalke D, Ackermann L. *ChemistryEurope*, 2025, 3: e202500071
114 Zhang Y, Yang C, Meng X, Wu M, Yang D, Song MP, Niu JL. *Org Lett*, 2025, 27: 6076–6081
115 Das A, Kumaran S, Maity P, Premkumar JR, Sundararaju B. *J Am Chem Soc*, 2025, 147: 26226–26237
116 Wu Y, Wang Z, Jia Z, Chen J, Huang F, Zhan B, Yao Q, Shi B. *Angew Chem Int Ed*, 2023, 62: e202310004
117 Li T, Shi L, Wang X, Yang C, Yang D, Song MP, Niu JL. *Nat Commun*, 2023, 14: 5271
118 Sun Y, Yang T, Wang Q, Shi L, Song MP, Niu JL. *Org Lett*, 2024, 26: 5063–5068
119 Cai J, Li L, Wang C, Qin S, Li Y, Liao SY, Wang S, Gao H, Zhou Z, Huang Y, Yi W, Zeng Z. *Green Chem*, 2024, 26: 11524–11530
120 Liu T, Zhang W, Xu C, Xu Z, Song D, Qian W, Lu G, Zhang CJ, Zhong W, Ling F. *Green Chem*, 2023, 25: 3606–3614
121 Lin Y, von Münchow T, Ackermann L. *ACS Catal*, 2023, 13: 9713–9723
122 Chen J, Teng M, Huang F, Song H, Wang Z, Zhuang H, Wu Y, Wu X, Yao Q, Shi B. *Angew Chem Int Ed*, 2022, 61: e202210106
123 Zhou G, Chen J, Yao Q, Huang F, Wang Z, Shi B. *Angew Chem Int Ed*, 2023, 62: e202302964
124 Das A, Kumaran S, Ravi Sankar HS, Premkumar JR, Sundararaju B. *Angew Chem Int Ed*, 2024, 63: e202406195
125 Xia X, Zheng C, Hang Y, Guo J, Liu T, Song D, Chen Z, Zhong W, Ling F. *Green Chem*, 2024, 26: 8323–8329
126 Jiang B, Wang H, Sun X, Qiao Y, Xu X, Miao Z. *Adv Synth Catal*, 2025, 367: e202500021
127 Yang D, Zhang X, Wang X, Si XJ, Wang J, Wei D, Song MP, Niu JL. *ACS Catal*, 2023, 13: 4250–4260
128 Yao Q, Huang F, Chen J, Zhong M, Shi B. *Angew Chem Int Ed*, 2023, 62: e202218533
129 von Münchow T, Liu Y, Parmar R, Peters SE, Trienes S, Ackermann L. *Angew Chem Int Ed*, 2024, 63: e202405423
130 Wang Z, Wu Y, Yao Q, Shi B. *Angew Chem Int Ed*, 2023, 62: e202304706
131 Wu YJ, Chen JH, Teng MY, Li X, Jiang TY, Huang FR, Yao QJ, Shi BF. *J Am Chem Soc*, 2023, 145: 24499–24505
132 Huang FR, Yao QJ, Zhang P, Teng MY, Chen JH, Jiang LC, Shi BF. *J Am Chem Soc*, 2024, 146: 15576–15586
133 Gandeepan P, Rajamalli P, Cheng C. *Angew Chem Int Ed*, 2016, 55: 4308–4311
134 Dey A, Volla CMR. *Org Lett*, 2021, 23: 5018–5023
135 Chen JH, Yao QJ, Zhong MY, Jiang TY, Huang FR, Li X, Shi BF. *ACS Cent Sci*, 2025, 11: 127–135
136 von Münchow T, Pandit NK, Dana S, Boos P, Peters SE, Boucat J, Liu YR, Scheremetjew A, Ackermann L. *Nat Catal*, 2025, 8: 257–269
137 Dana S, Pandit NK, Boos P, von Münchow T, Peters SE, Trienes S, Haberstock L, Herbst-Irmer R, Stalke D, Ackermann L. *ACS Catal*, 2025, 15: 4450–4459
138 Teng M, Liu D, Mao S, Wu X, Chen J, Zhong M, Huang F, Yao Q, Shi B. *Angew Chem Int Ed*, 2024, 63: e202407640
139 Mei M, Zhang Y. *Chin J Org Chem*, 2024, 44: 3263–3264
140 Das A, Mandal R, Ravi Sankar HS, Kumaran S, Premkumar JR, Borah D, Sundararaju B. *Angew Chem Int Ed*, 2024, 63: e202315005
141 Xu Y, Lin Y, Homölle SL, Oliveira JCA, Ackermann L. *J Am Chem Soc*, 2024, 146: 24105–24113
142 Li T, Zhang Y, Du C, Yang D, Song MP, Niu JL. *Nat Commun*, 2024, 15: 7673
143 Qian P, Zhou G, Hu J, Wang B, Jiang A, Zhou T, Yuan W, Yao Q, Chen J, Kong K, Shi B. *Angew Chem Int Ed*, 2024, 63: e202412459
144 Zhang L, Yang C, Wang X, Yang T, Yang D, Dou Y, Niu JL. *Green Chem*, 2024, 26: 10232–10239
145 Huang FR, Zhang P, Yao QJ, Shi BF. *CCS Chem*, 2024, 6: 2783–2793
146 Huang F, Teng M, Qiu H, Yao Q, Shi B. *Angew Chem Int Ed*, 2025, 64: e202506465
147 Xu Y, Pandit NK, Meraviglia S, Boos P, Stark PAM, Surke M, Herbst-Irmer R, Stalke D, Ackermann L. *ACS Catal*, 2025, 15: 11716–11725